

AD A047491

DDC FILE COPY

REPORT DOCUMENTATION PAGE		READ INSTRUCTIONS BEFORE COMPLETING FORM
1. REPORT NUMBER <b>19</b> <b>AFOSR-TR-77-1277</b>	2. GOVT ACCESSION NO.	3. RECIPIENT'S CATALOG NUMBER
4. TITLE (and Subtitle) <b>STATISTICAL ANALYSIS OF STEADY STATE COMBUSTION OF NONMETALLIZED COMPOSITE SOLID PROPELLANTS.</b>		5. TYPE OF REPORT & PERIOD COVERED <b>7 INTERIM</b> <b>1 Jul 76 - 30 Sep 77</b>
6. AUTHOR(s) <b>R L GLICK</b> <b>10</b>		7. PERFORMING ORG. REPORT NUMBER <b>14 U-77-08</b>
8. PERFORMING ORGANIZATION NAME AND ADDRESS <b>THIOKOL CORPORATION HUNTSVILLE DIVISION HUNTSVILLE, ALABAMA 35807</b>		9. CONTRACT OR GRANT NUMBER(s) <b>15 F49620-76-C-0008</b>
10. CONTROLLING OFFICE NAME AND ADDRESS <b>AIR FORCE OFFICE OF SCIENTIFIC RESEARCH/NA BLDG 410 BOLLING AIR FORCE BASE, D C 20332</b>		11. PROGRAM ELEMENT PROJECT, TASK AREA & WORK UNIT NUMBERS <b>16 2308</b> <b>17 A1</b> <b>61102F</b>
12. MONITORING AGENCY NAME & ADDRESS (if different from Controlling Office)		12. REPORT DATE <b>1977</b> <b>11 30 Sep 77</b>
		13. NUMBER OF PAGES <b>55</b> <b>12 56p</b>
		14. SECURITY CLASS. (of this report) <b>UNCLASSIFIED</b>
		15. DECLASSIFICATION/DOWNGRADING SCHEDULE
16. DISTRIBUTION STATEMENT (of this Report)  <b>Approved for public release; distribution unlimited.</b>		
17. DISTRIBUTION STATEMENT (of the abstract entered in Block 20, if different from Report)		
18. SUPPLEMENTARY NOTES		
19. KEY WORDS (Continue on reverse side if necessary and identify by block number) <b>STEADY-STATE COMBUSTION MODAL PROPERTIES DATA ANALYSIS CORRELATION OF DATA BASES COMBUSTION MODELING</b>		
20. ABSTRACT (Continue on reverse side if necessary and identify by block number) <b>The combustion model including aluminum and iron oxide was employed to correlate data bases of Miller and Maykut. Results for additive free formulations were excellent for both rate and exponent; results for formulations with aluminum and aluminum plus iron oxide were poor. A new method for extracting particle size dependent information from rate/response function/formulation data was developed from the statistical methodology itself and employed to process the aforementioned data bases. Results were encouraging; Miller's additive free and aluminum plus iron oxide data correlated very well; Millers aluminum data showed</b>		

**401944**

that the increasing aluminum particle size increases interactions between oxidizer modes; Maykut's data base showed that aluminum induced interactions among oxidizer modes are decreased as iron content increases. Results elucidate mechanisms for rate, exponent, and response function control and show that the equal rate hypothesis employed in much combustion modeling is incorrect. A new approach for including the effects of transients introduced by particle size dependent rates in both steady and nonsteady combustion modeling was conceived.

UNCLASSIFIED

AFOSR-TR- 77 - 1277

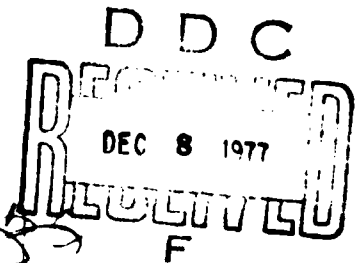
CONTROL NO. U-77-08

STATISTICAL ANALYSIS OF STEADY STATE COMBUSTION  
OF NONMETALLIZED COMPOSITE SOLID PROPELLANTS

DR. R. L. GLICK  
THIOKOL CORPORATION  
HUNTSVILLE, ALABAMA 35807

REPORT, CONTRACT F49620-76-C-0008

JULY 1, 1976 - SEPTEMBER 30, 1977



PREPARED FOR:

DEPARTMENT OF THE AIR FORCE  
AIR FORCE OFFICE OF SCIENTIFIC RESEARCH (AFSC)  
BOLLING AIR FORCE BASE, D. C. 20332

Approved for public release;  
distribution unlimited.

## NOTICE


Research sponsored by the Air Force Office of Scientific Research (AFSC), United States Air Force, under Contract F49620-76-C-0008. The United States Government is authorized to reproduce and distribute reprints for governmental purposes notwithstanding any copyright notation hereon.

## FOREWORD


This is a ~~SECRET~~ report covering the work completed under Contract F49620-76-C-0008 for the period 1 July 1976 through 30 September 1977. Publication of this report does not constitute Air Force approval of the findings or conclusions contained herein. It is published only for the exchange of data and stimulation of ideas.

APPROVED BY:

  
G. F. Mangum  
Project Director

  
C. C. Lee  
Director, Programs

AIR FORCE OFFICE OF SCIENTIFIC RESEARCH (AFSC)  
NOTICE OF TRANSMITTAL TO DDC  
This technical report has been reviewed and is  
approved for public release IAW AFR 190-12 (7b).  
Distribution is unlimited.  
A. D. BLOSE  
Technical Information Officer

ACCESSION for	
NTIS	Write Section <input checked="" type="checkbox"/>
DDC	Index <input type="checkbox"/>
UNANIMOUS	
JUST	
BY	
DISTRICT	
D.	
	

## CONTENTS

	<u>Page No.</u>
ABSTRACT	3
INTRODUCTION	4
TECHNICAL DISCUSSION	6
Combustion Modeling	6
Analysis of Data with the Statistical Framework	7
Strategy for Inclusion of Nonsteady Phenomena in Combustion Modeling	11
REFERENCES	12
APPENDICES	
A. Nomenclature	37
B. Modal Properties Code	39
FIGURES	
1. Burning Rate: Calculated vs Experimental for Miller's 24 micron Aluminum Additive Data Base (SD-I-88)	13
2. Burning Rate Exponent: Calculated vs Experimental for Miller's 24 micron Aluminum Additive Data Base (SD-I-88)	14
3. Burning Rate: Calculated vs Experimental for Miller's 24 micron Aluminum plus 1% Iron Oxide Data Base (SD-VII-88)	15
4. Burning Rate Exponent: Calculated vs Experimental for Miller's 24 micron plus 1% Iron Oxide Data Base (SD-VII-88)	16
5. Burning Rate: Calculated vs Experimental for Maykut's Data Base	17
6. Burning Rate Exponent: Calculated vs Experimental for Maykut's Data Base	18
7. Burning Rate: Calculated vs Experimental for Miller's Additive Free Data Base (SD-III-88)	19

Figures (continued)

	<u>Page No.</u>
8. Exponent: Calculated vs Experimental for Miller's Additive Free Data Base (SD-III-88)	20
9. Burning Rate: Calculated vs Experimental for Miller's 18% 24-micron Aluminum Data Base (SD-I-88)	21
10. Burning Rate Exponent: Calculated vs Experimental for Miller's 24 micron Aluminum Additive Data Base (SD-I-88)	22
11. Burning Rate: Calculated vs Experimental for Miller's 90 micron Aluminum Additive Data Base (SD-IV-88)	23
12. Burning Rate Exponent: Calculated vs Experimental for Miller's 90 micron Aluminum Additive Data Base (SD-IV-88)	24
13. Burning Rate: Calculated vs Experimental for Miller's 6 micron Aluminum Additive Data Base (SD-V-88)	25
14. Exponent: Calculated vs Experimental for Miller's 6 micron Aluminum Additive Data Base (SD-V-88)	26
15. Burning Rate: Calculated vs Experimental for Miller's Extended Solids Data Base (SD-VI-90)	27
16. Burning Rate Exponent: Calculated vs Experimental for Miller's Extended Solids Data Base (SD-VI-90)	28
17. Burning Rate: Calculated vs Experimental for Miller's 24 micron Aluminum/Iron Oxide Data Base (SD-VII-88)	29
18. Exponent: Calculated vs Experimental for Miller's 24 micron Aluminum/Iron Oxide Data Base (SD-VII-88)	30
19. Variation of Modal Rates with Modal D <sub>43</sub> (microns) for Miller's Additive Free Data Base (SD-III-88)	31
20. Effect of Volume Mean Diameter on Burn Rate, Miller's Data Base (SD-VII-88)	32
21. Effect of Volume Mean Diameter on Exponent, Miller's Data Base (SD-VII-88)	33
22. Schematic Illustrating Arrangement of Pseudopropellants	34

## ABSTRACT

The combustion model including aluminum and iron oxide was employed to correlate data bases of Miller and Maykut. Results for additive free formulations were excellent for both rate and exponent; results for formulations with aluminum and aluminum plus iron oxide were poor. A new method for extracting particle size dependent information from rate/response function/formulation data was developed from the statistical methodology itself and employed to process the aforementioned data bases. Results were encouraging; Miller's additive free and aluminum plus iron oxide data correlated very well; Miller's aluminum data showed that increasing aluminum particle size increases interactions among oxidizer modes; Maykut's data base showed that aluminum induced interactions among oxidizer modes are decreased as iron content increases. Results elucidate mechanisms for rate, exponent, and response function control and show that the equal rate hypothesis employed in much combustion modeling is incorrect. A new approach for including the effects of transients introduced by particle size dependent rates in both steady and nonsteady combustion modeling was conceived.

Goals of embedding Williams/Guirao AP decomposition model and Cohen nitramine model in the combustion model were not reached.

## INTRODUCTION

Increasing emphasis on low visible exhaust signature in tactical applications of solid rocket motors has virtually eliminated significant amounts of condensed phases from the products of combustion. This has created a number of problems.

1. At equal total solids contents replacement of metal additive with AP reduces specific impulse.
2. Replacement of metal additive with oxidizer alters the relationship among rate, formulation, and environment.
3. Replacement of metal additive with oxidizer increases the probability of combustion instability because particle damping is absent.

The upshot is that propellant formulation is more difficult in the low signature area; all constraints imposed on a high signature formulation must be met at a higher total solids loading (if equivalent energetics are demanded) with greatly enhanced probability of combustion instability plus a new constraint-signature.

Propellant formulation has long proceeded in largely empirical channels. However, deviations of low signature formulations from the rate/formulation/environment relations established largely for metallized propellants over the past two decades, introduction of ingredients outside the historical data base (nitramines, ultra fine aluminum oxide, etc), and the importance of combustion instability have all contributed to increasing cost and risk of low signature propellant development efforts relative to those for similar high signature propellants. The economics of an empirical approach are strongly related to the cost of gathering data. With high signature systems only passing attention was paid to combustion stability; this is not the case for low signature systems. As a result, determination of propellant properties related to combustion stability accounts for a substantial portion of the aforementioned cost/risk differential.

Theory<sup>(1)</sup> shows that steady and nonsteady combustion phenomena are related for homogeneous propellants when the frequency is not too high. On phenomenological grounds a steady/nonsteady relation must also exist for composite propellants. However, it is not that for homogeneous propellants.<sup>(2)</sup> Since a steady/nonsteady relation means that propellant stability properties can be computed from steady-state data, it would be of considerable economic importance for low signature composite propellant development programs. Unfortunately, the empirical path followed by propellant developers virtually prohibits any possibility for discerning the aforementioned steady/nonsteady relation.



The overall objective of this work is to construct an analytical model describing steady-state combustion of composite propellants. This is both a worthy goal in itself (propellant constraints relate to steady-state properties) and a necessary step to understanding nonsteady phenomena.

## TECHNICAL DISCUSSION

### Combustion Modeling

Reference 3 presents mathematical developments for a steady-state combustion model of composite propellant with additives. Basically, a statistical procedure is employed to account for oxidizer particle size and additives are divided into either active or passive categories. In the former category, the additive modifies the kinetics of the deflagration process; in the latter the additive acts solely as an inert heat sink. In this program this model has been transformed into an operational computer code and employed to correlate experimental data.

The data bases of Miller<sup>(4)</sup> and Maykut<sup>(5)</sup> have been employed to test the model. Miller's data base includes additive free, aluminum additive, and aluminum plus iron oxide additives. Maykut's data base includes aluminum and varying amounts of iron oxide. Both data bases are for HTPB/AP formulations and have similar total solids contents.

The correlation process proceeded as follows. First, basic parameters were adjusted to give a "best" fit with Miller's additive free data. Second, with these parameters, rates and exponents were predicted for Miller's 24 micron aluminum additive formulations (no additional parameters are required to account for passive additives). Third, parameters associated with the iron oxide catalyst were adjusted to give a best fit to selected rate vs catalyst data in Maykut's data base. Fourth, rates and exponents were predicted for the formulations in Miller's 24 $\mu$  aluminum plus 1% iron oxide data base and the remainder of Maykut's data base.

Results for Miller's additive free data are reported elsewhere.<sup>(6)</sup> The correlation was superb for both rate and exponent. The standard error of estimate of the correlation was roughly 6 percent. This is of the same order as errors in the burning rate measurements themselves. Consequently, the correlation is essentially as good as the data itself.

Figures 1 and 2 present the correlation of Miller's 24 micron aluminum data (formulation set SD-I-88). It is clear that appreciable scatter exists. Examination of the outliers\* shows that, in general, they are formulations possessing a "wide" distribution. Consequently, the present model seems adequate only for metallized propellants with narrow distributions. As Miller has pointed out elsewhere<sup>(7)</sup>, the addition of aluminum causes interactions to occur among particles of differing size. As presently constituted, the combustion model does not include interactions.

---

\*Numbers associated with the formulations are the formulation numbers assigned by Miller.<sup>(4)</sup>

Figures 3 and 4 present the correlation of Miller's 24 micron aluminum plus 1% iron oxide data (formulation set SD-VII-88). There is considerable scatter in this correlation. However, when contrasted with the aforementioned aluminum additive data the scatter does not appear to relate to wide and narrow distributions. Indeed, it appears that there is a systematic error in the predicted exponents (refer to the dashed correlation line) and that propellants with rates below 1 in/sec systematically deviate from the above 1 in/sec correlation. The latter behavior was evident in correlations of the same data presented by Beckstead.<sup>(8)</sup>

Figures 5 and 6 present the correlation of Maykut's HTPB/AP/30 $\mu$  Al/iron oxide data base. As before, there is appreciable scatter. However, the character of the scatter differs from that of Miller's 24 $\mu$  Al plus iron oxide data base. Here the outliers are largely those with wide distributions. Moreover, the rate correlation possesses a systematic deviation (dashed line) while the exponent correlation doesn't.

In summary, correlation of these systematic data bases has shown that the basic additive free model appears to be adequate while the model for additives is inadequate. It is clear that metal additives cannot be treated as simple heat sinks. However, problems with the present treatment of catalysts are confounded with aluminum effects. An extensive catalyst data base without metal additive is required to adequately define inadequacies in the catalyst model.

#### Analysis of Data With the Statistical Framework

The aforementioned results show that the present combustion model is, at present, inadequate for quantitative calculations with propellants containing additives. In the combustion model errors can arise from two sources (a) the statistical framework and (b) the unit combustion model. One suspects that the statistical framework is more accurate than the unit combustion model. Therefore, effort was expended to explore use of the basic statistical framework to correlate data.

Correlation of Miller's additive free data had shown that best correlation occurs when the pseudo-propellant oxidizer/fuel ratios are all equal. Thus,  $\alpha_{ox,k}^* = \alpha_{ox}$  so that the basic rate equation

$$\bar{m}_k = \oint_D (\bar{m}_0 / \alpha_{ox,k}^*) \sum_{k=1}^M \alpha_{ox,k} F_{ox,k} dD/D \quad (1)$$

becomes

$$\bar{m}_k = \alpha_{ox}^{-1} \sum_{k=1}^M \alpha_{ox,k} \oint_D \bar{m}_0 F_{ox,k} dD/D \quad (2)$$

The integral in the latter equation is the mean mass flux from the pseudo-propellant containing the kth oxidizer mode. Therefore, Eq. (2) can be

rewritten as

$$\bar{m}_x = \alpha_{ox}^{-1} \sum_{k=1}^M \alpha_{ox,k} \bar{m}_k \quad (3)$$

which leads to

$$\bar{r}_x = \alpha_{ox}^{-1} \sum_{k=1}^M \alpha_{ox,k} \bar{r}_k \quad (4)$$

since  $\alpha_{ox,D}^* = \alpha_{ox}$ . Differentiation of Eq. (4) leads to

$$d\bar{r}_x = \alpha_{ox}^{-1} \sum_{k=1}^M \alpha_{ox,k} \bar{r}_k d\bar{r}_k / \bar{r}_k \quad (5)$$

Therefore, algebraic manipulation yields

$$\bar{m}_x = (\alpha_{ox} \bar{r}_x)^{-1} \sum_{k=1}^M \alpha_{ox,k} \bar{r}_k \bar{m}_k \quad (6)$$

$$\bar{\sigma}_{p,x} = (\alpha_{ox} \bar{r}_x)^{-1} \sum_{k=1}^M \alpha_{ox,k} \bar{r}_k \bar{\sigma}_{p,k} \quad (7)$$

$$\bar{R}_{p,x} = (\alpha_{ox} \bar{r}_x)^{-1} \sum_{k=1}^M \alpha_{ox,k} \bar{r}_k \bar{R}_{p,k} \quad (8)$$

These equations assert that the ballistic properties of composite propellants should be expressible in terms of modal properties. On the other hand, experimental data can be analyzed to determine these modal properties. That is, if ballistic data from at least  $N$  formulations with the same chemical composition but differing median oxidizer size were available, the  $\bar{r}_k$ ,  $\bar{n}_k$ , etc ( $k=1, N$ ) could be computed from that data. Once these  $\bar{r}_k$ ,  $\bar{n}_k$ , etc ( $k=1, N$ ) were known, the ballistic properties of any formulation with that chemical composition could be computed. Consequently, ballistic properties of all members of a bimodal family with fixed chemical composition but differing particle size could be defined from ballistic data for just two members; a trimodal family would require data from three members.

In short, it appears that the statistical framework offers some exciting possibilities for generalizing experimental ballistic data. In addition, the modal pseudo-propellant properties demonstrate the effects of particle size and additives at a level much closer to the unit combustion model. Therefore, the "statistical framework approach" also offers some exciting possibilities for assisting the theoretical modeling.

To test the "accuracy" of the statistical framework for correlating ballistic data a computer code for extracting the best, in a statistical sense,

$\bar{r}_k, \bar{n}_k$  from any data set was developed. Appendix B presents the code and a sample case illustrating input and output. Figures 7 and 8 present the correlation of Miller's additive free rate and pressure exponent data while Table 1 presents the best fit  $\bar{r}_k$  and  $\bar{n}_k$ . Correlation in all cases is superb.

Figures 9 and 10 present the correlation of Miller's 24 micron aluminized propellant data while Table 1 presents the best fit  $\bar{r}_k$  and  $\bar{n}_k$ . The presence of aluminum degrades the correlation. However, data scatter is much less than that shown by Figures 1 and 2. Therefore, an appreciable portion of the inaccuracy in the theoretical model must be attributable to the unit combustion model. It is important to note that the data outliers are generally associated with formulations possessing wide oxidizer distributions. Consequently, there is every reason to believe that if interaction effects were included in the statistical framework the outliers would be brought into the fold.

Figures 11 to 14 present correlations for Miller's 6 micron and 90 micron aluminized propellant data while Table 1 presents the best fit  $\bar{r}_k$  and  $\bar{n}_k$ . Comments pertinent to the individual data correlation are essentially the same as those for the 24 micron data. However, when Figures 9, 11, and 13 are viewed in sequence it is obvious that the correlation degrades with increasing aluminum particle size. This trend is also evident in the standard error of estimate data of Table 1. Thus, interaction effects must increase with increasing aluminum particle size.

Figures 15 and 16 present correlations for Miller's 24 micron plus 1 percent iron oxide propellant data while Table 1 presents the best fit  $\bar{r}_k$  and  $\bar{n}_k$ . Correlation of this data is superb. Clearly, as Miller has noted, the addition of 1% iron oxide has suppressed (or compensated for) interactions among the oxidizer particles.

Table II presents modal rates and exponents and statistical measures of the correlation of Maykut's data base. Several trends are noted. First, the correlation improves as pressure decreases. This suggests that interactions are related to transport property effects since kinetics become of increasing importance as pressure decreases. Second, the correlation improves as catalyst content increases. This shows that catalyst progressively cancels (or compensates) interactions. Note that in Miller's data 1% catalyst eliminated interactions while 2% catalyst is required here. Third, note that catalyst has little effect on the 16 $\mu$  mode; effects appear to be concentrated in the coarse and fine modes.

The above results show that the correlation methodology possesses excellent capabilities for extracting modal properties under circumstances when interactions are small. Data from these situations may be employed to elucidate particle dependent combustion phenomena. Figure 19 presents the variation of modal burning rate with volume mean particle size for Miller's additive free formulations. It is clear that burning rate depends strongly upon oxidizer particle size and that variation is pressure dependent. Note that at 500 psi there is little variation of rate with particle size for particles

below  $10\mu$ . This indicates that small particle rates are kinetic rather than diffusion limited. Note that this situation alters as pressure increases. Figure 20 compares the diametral dependence of burning rate with formulation for Miller's data base. The addition of aluminum substantially degrades the burning rates of fine material while producing relatively little effect on the coarse modes. The addition of catalyst causes substantial increases in the burning rate of both fine and coarse AP modes but little effect in the 50 to  $100\mu$  range. Figure 21 illustrates the dependence of modal exponent on volume mean diameter of the mode for several formulations in Miller's data base. For the additive free formulation exponent increases to unity as diameter decreases. This indicates that as diameter approaches zero rate control shifts to a kinetic mechanism. The surprising result is the tendency for exponent to increase for very coarse oxidizer modes. The mechanism for this increase is not known. However, the combustion model predicts this trend.<sup>(6)</sup> The effect of both aluminum and catalyst is primarily to suppress high exponents at small particle sizes.

The modal property trends shown in Figures 20 and 21 explain many formulation trends. For example, rate is sensitive to the amount of coarse material because rate is weighted solely by mass fraction. However, exponent is much less sensitive to the amount of coarse material because the exponent is weighted by both mass fraction and rate and the modal rates of coarse material are low. Thus, rate tends to be controlled by both coarse and fine while exponent is largely controlled by the fine fraction. With the data in hand it is clear that high exponent ( $n > 0.7$ ) formulations with significant metal content are highly improbable in a HTPB/AP/Al/Iron Oxide system; the modal exponents are all low. On the other hand, high exponent can be readily achieved in an additive free system simply by incorporating small diameter fines.

It appears that inert additives act to suppress both rate and exponent of fine AP. Rate can be restored with a catalytic additive, but exponent apparently cannot. This suggests that inert additives should provide means for reducing exponent independent of particle size control while a mixture of inert/catalytic additives should provide means for controlling both rate and exponent independent of particle size control.

The functional similarity of Eqs. 6 and 8 and the fact that  $\bar{R}_{p,t}$  approaches  $\bar{n}_t$  as frequency approaches zero suggests strongly that techniques for exponent control should carry over into control of pressure coupled response. From the arguments presented above it is seen that propellants formulated with significant amounts of coarse AP should possess both low exponent and low pressure coupled driving. Moreover, inert additives should be excellent stability additives. These trends have substantially been borne out.<sup>(10)</sup> The efficacy of inert additives has generally been laid at the doorstep of particle damping. However, the above suggests that part of the observed effects may be attributed to reduced pressure coupled driving.

It is important to note that the  $R_p$ ,  $n$  "analogy" is definitely not exact. The reason is that the frequency where the response function peaks varies with

the thickness of the subsurface energy store which varies locally with rate. What this means is that dynamic effects cloud the issue. Therefore, the above formulation generalizations will probably vary with frequency.

It is unfortunate that available data bases do not usually contain either temperature sensitivity or response function information (Miller's data base will eventually supply limited response function information). Without systematic data in these areas we are simply working in the dark.

#### Strategy for Inclusion of Nonsteady Phenomena in Combustion Modeling

Combustion phenomena in composite propellants is inherently nonsteady at the single particle level. That is, even when the environment is quiescent  $r = r(x, t)$  where  $x$  denotes position on the burning surface. This, in turn, implies that  $T_g = T_g(x, t)$  and  $q''_g = q''_g(x, t)$ . However, all steady-state combustion models are functionally equivalent to the assumption that  $q''_g$  and  $T_g$  are not functions of time. This is justified by assuming that transient phenomena cancels in the summation to a mean state. If the mean state is to be one of the accessible physical states, this assumption is generally false; the magnitude of the error introduced by this assumption is unknown.

The success of the steady-state models in dealing with Miller's additive free formulations suggests (but does not prove) that when the environment is quiescent these errors are small. However, in models that employ the equal rate hypothesis  $r(D) = r(D + \Delta D)$  surface temperature, subsurface energy store, and surface heat flux are equivalent for all particles. Consequently, for low and midfrequency response where the chemically reactive zones behave quasi-steadily, the response function should possess characteristics similar to those of a homogeneous propellant (single relative maximum). On the other hand, if  $r(D) \neq r(D + \Delta D)$  surface temperature and heat flux are not unique. Therefore, the possibility of a multi-relative maximum response function exists. The factor that distinguishes among these possibilities is the subsurface temperature profile.

In existing nonsteady models approximations have been introduced. Condon and Glick<sup>(2)</sup> have assumed that each monodisperse pseudo-propellant in the set representing the composite propellant possesses its equilibrium subsurface temperature profile. Cohen<sup>(9)</sup> has introduced the particle diameter as a length scale and thereby assumed the characteristic thermal thickness is proportional to particle size. Results depend strongly upon these assumptions.<sup>(2)</sup>

The major difficulty with current approaches to the condensed phase heat transfer aspects of the composite propellant combustion problem is that they are deterministic when the physical problem has a probabilistic character. For steady-state probabilistic phenomena probabilities in the spatial domain at fixed time are equivalent to probabilities in the temporal domain at fixed spatial coordinates. Thus, in a one-dimensional sense the propellant can be viewed as a super Dagwood sandwich of the monodisperse pseudo-propellants (refer to Figure 22). As the monodisperse pseudo-propellants all possess

the same bulk thermal properties in the mean, these properties are common to the sandwich layers. Therefore, the temperature field is governed by

$$\partial T / \partial t = \kappa \partial^2 T / \partial y^2 - r \partial T / \partial y \quad (6)$$

The initial condition is clearly

$$T(-\infty, t) = T_0 \quad (7)$$

Following Z-N<sup>(1)</sup> appropriate boundary "conditions" that enable computation of  $r(t)$  are

$$r = r(q''_{\bar{g}}, p, D) \quad (8)$$

$$T_g = T_g(q''_{\bar{g}}, p, D) \quad (9)$$

$$p = p(t) \quad (10)$$

In conventional Z-N strategy  $r$  and  $T_g$  are not functions of particle diameter because conventional Z-N strategy applies solely to homogeneous propellants. Since deflagration occurs through a layered medium here the additional independent variable must occur.\*

The Z-N boundary conditions can be derived from any steady-state source since the Z-N form of the boundary conditions is independent of time as long as the reactive regions are quasi-steady. The obvious source is from a detailed combustion model. However, by employing the aforementioned methodology to extract modal properties from experimental data a source much closer to basic experimental data may be available. The latter approach is in the original spirit of Z-N methodology which was aimed at circumventing need for combustion modeling.

The last question to be answered is how are the pseudo-propellant layers arranged. The answer of course is randomly such that the probability of finding pseudo-propellant with  $D \leq D \leq D+dD$  is equivalent to the volume fraction of that pseudo-propellant in the propellant recipe. This is the probabilistic aspect of the problem.

The output of this approach for a small sinusoidal environment variation will be both the mean burning rate and the small signal response to that variation (pressure coupled response function). In addition, mean rates and small signal response functions for each pseudo-propellant should be recoverable.

---

\*The methodology can also account for velocity coupling.<sup>(1)</sup>



## REFERENCES

1. Novozhilov, B.V., "Nonstationary Combustion of Solid Rocket Fuels", FTD-MT-24-317-74, 1974.
2. Condon, J.A., Osborn, J.R., and Glick, R.L., "Statistical Analysis of Polydisperse, Heterogeneous Propellant Combustion", CPIA Publication 281, Vol. II, pp. 209-224, 1976.
3. Glick, R.L., "Mean Flow/Acoustic Interactions and Statistical Analysis of Steady-State Combustion of Nonmetallized Composite Solid Propellants", Final Report, Contract F44620-74-C-0080 (1976).
4. Miller, R.R., et al., "The Control of Solid Distribution in HTPB Propellants", Final Report, Contract AFRPL 04611-76-C-0006, in preparation.
5. Webb, G.E., Low Cost Propellant Development Program, Monthly Report, Contract DAAH01-76-C-0170, (Thiokol Control No. U-76-424A), August 1976.
6. Renie, J.P., Condon, J.A., and Osborn, J.R., "Oxidizer Size Distribution Effects on Pressure and Temperature Sensitivity", 14th JANNAF Combustion Meeting, 1977.
7. Miller, R.R. and Martin, J.R., "Control of Solids Distribution III--The Effects of Al Particle Size and Iron Oxide Addition on the Ballistics of HTPB Propellants", presented at 14 JANNAF Combustion Meeting, 1977.
8. Beckstead, M.W., "A Model for Solid Propellant Combustion", presented at 14th JANNAF Combustion Meeting, 1977.
9. Cohen, N.S., et al., "Design of a Smokeless Solid Rocket Motor Emphasizing Combustion Stability", CPIA Publication 273, Vol. II, pp. 205-220, 1975.
10. Cohen, N.S., "Workshop Report: Combustion Instability of Smokeless Propellants", presented at 14th JANNAF Combustion Meeting, Aug. 1977.

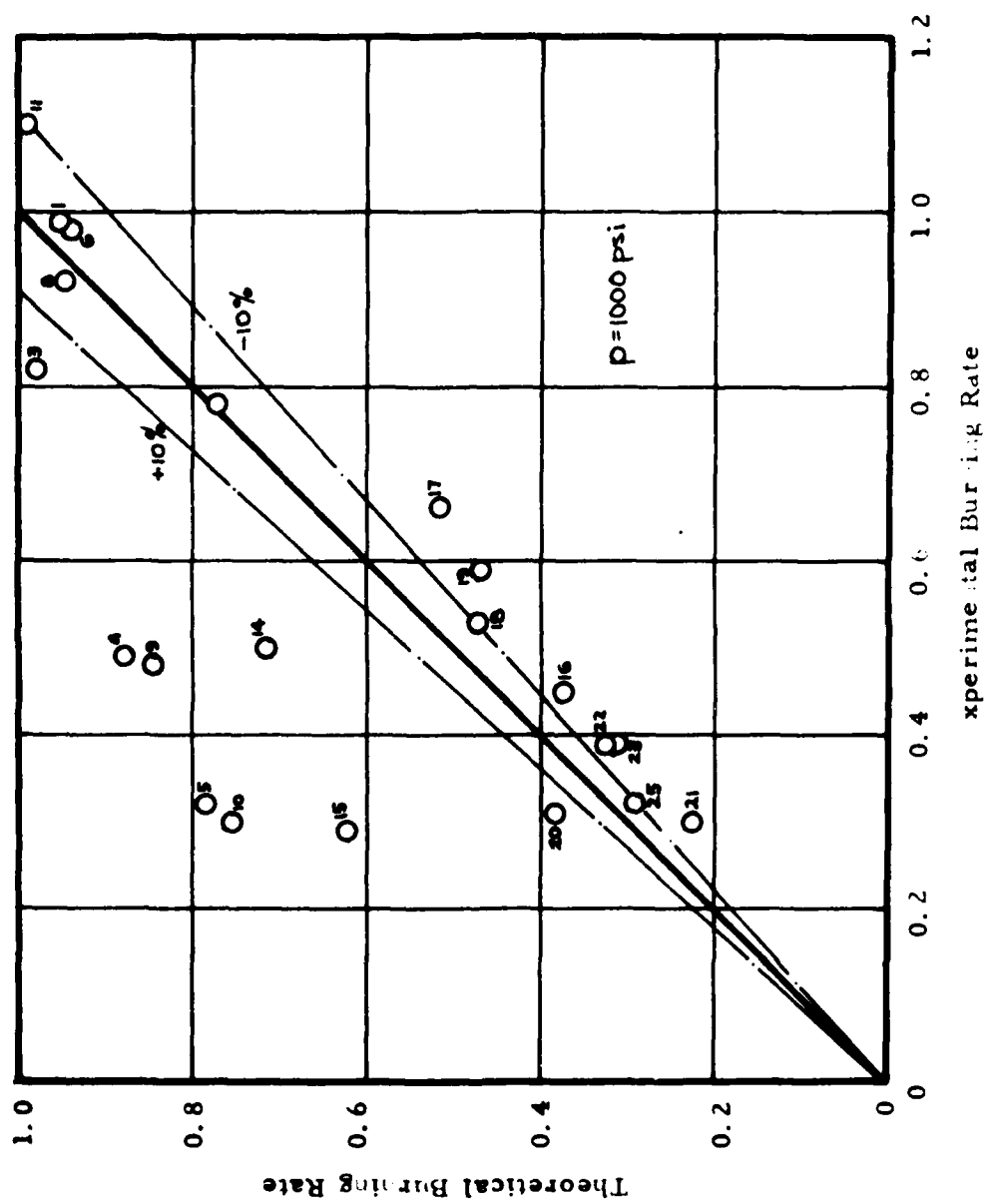


Figure 1. Burning Rate: Calculated versus Experimental for Miller's 24 micron Aluminum Additive Data Base (SD-I-88)

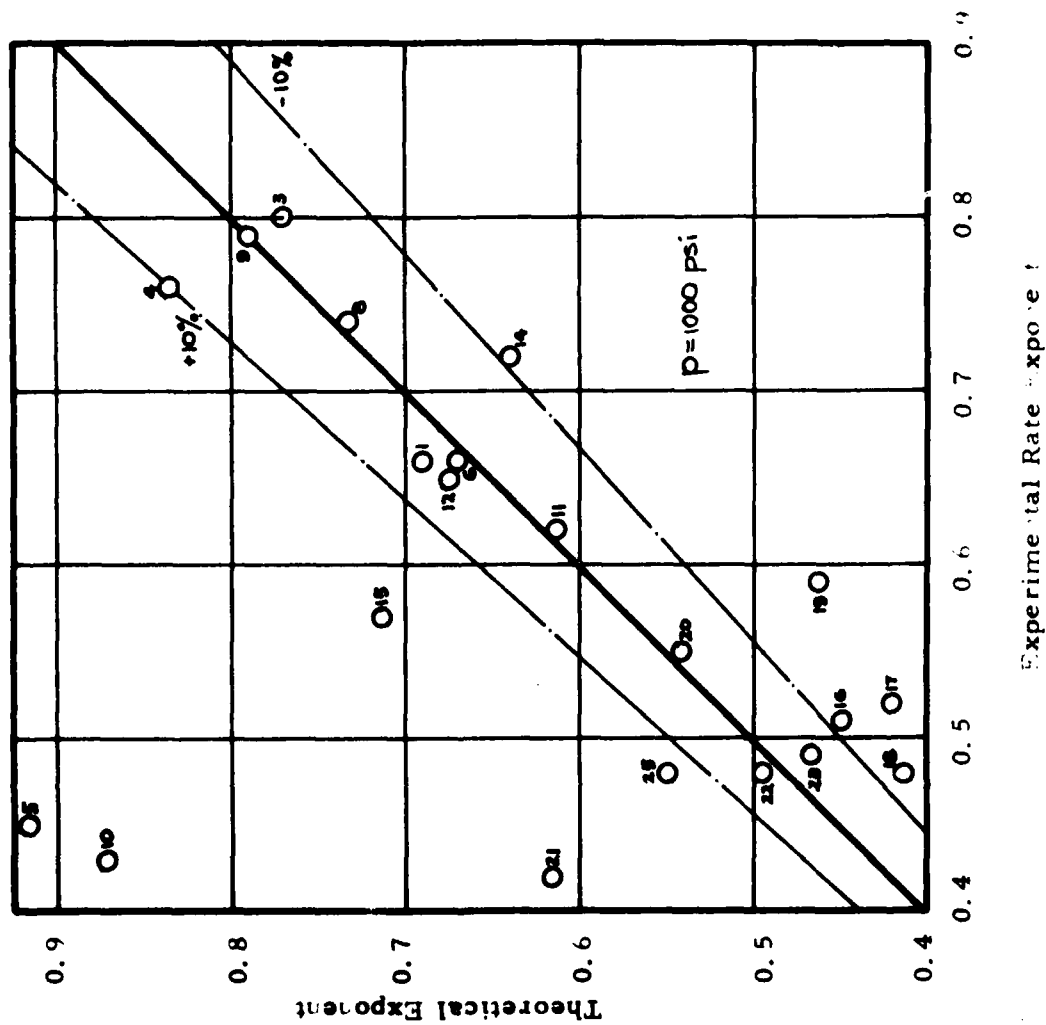


Figure 2. Burning Rate Exponent: Calculated versus Experimental for Miller's 24 micron Aluminum Additive Data Base (SD-1-88)

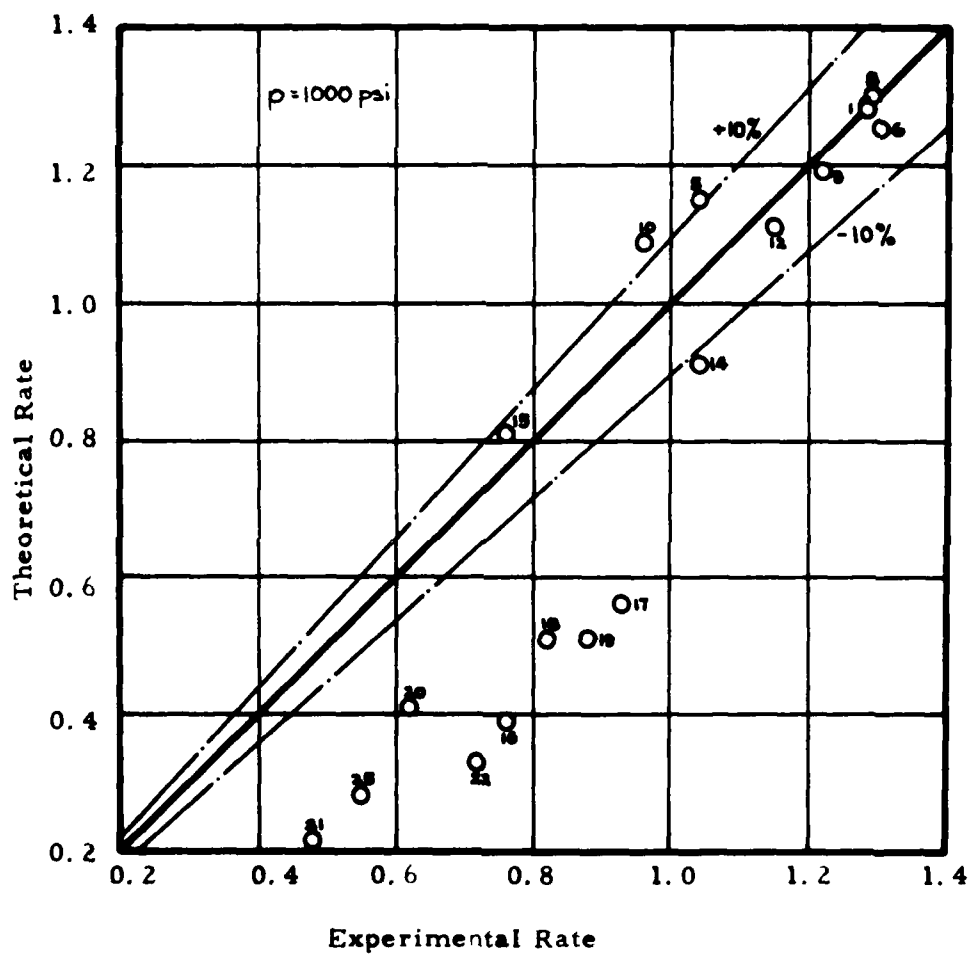


Figure 3. Burning Rate: Calculated versus Experimental for Miller's 24 micron Aluminum plus 1% Iron Oxide Data Base (SD-VII-88)

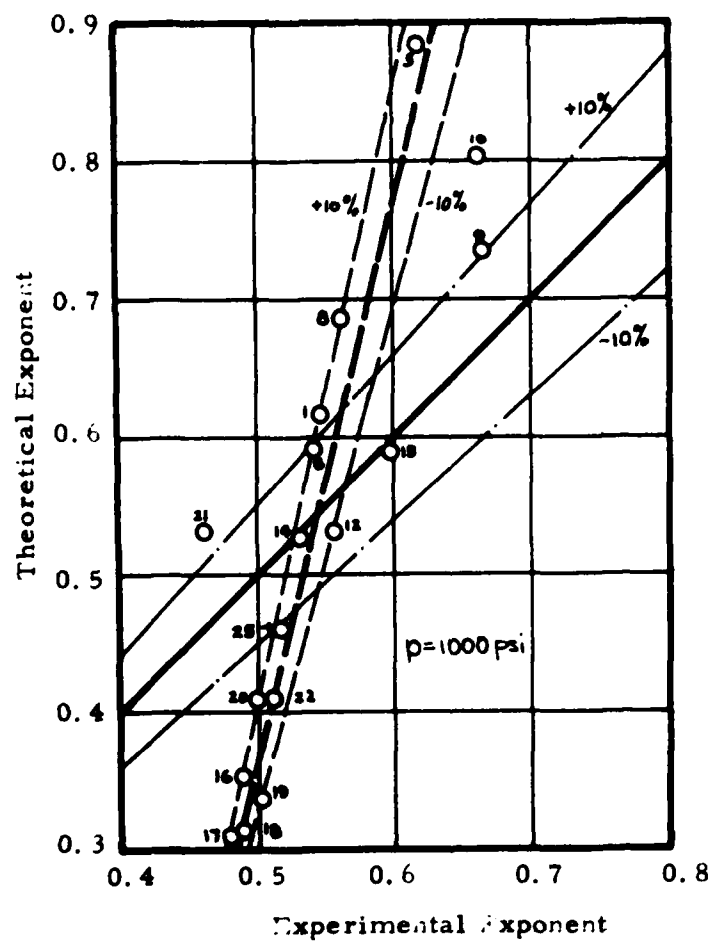


Figure 4. Burning Rate Exponent: Calculated versus Experimental for Miller's 24 micron plus 1% Iron Oxide Data Base (SD-VII-88)

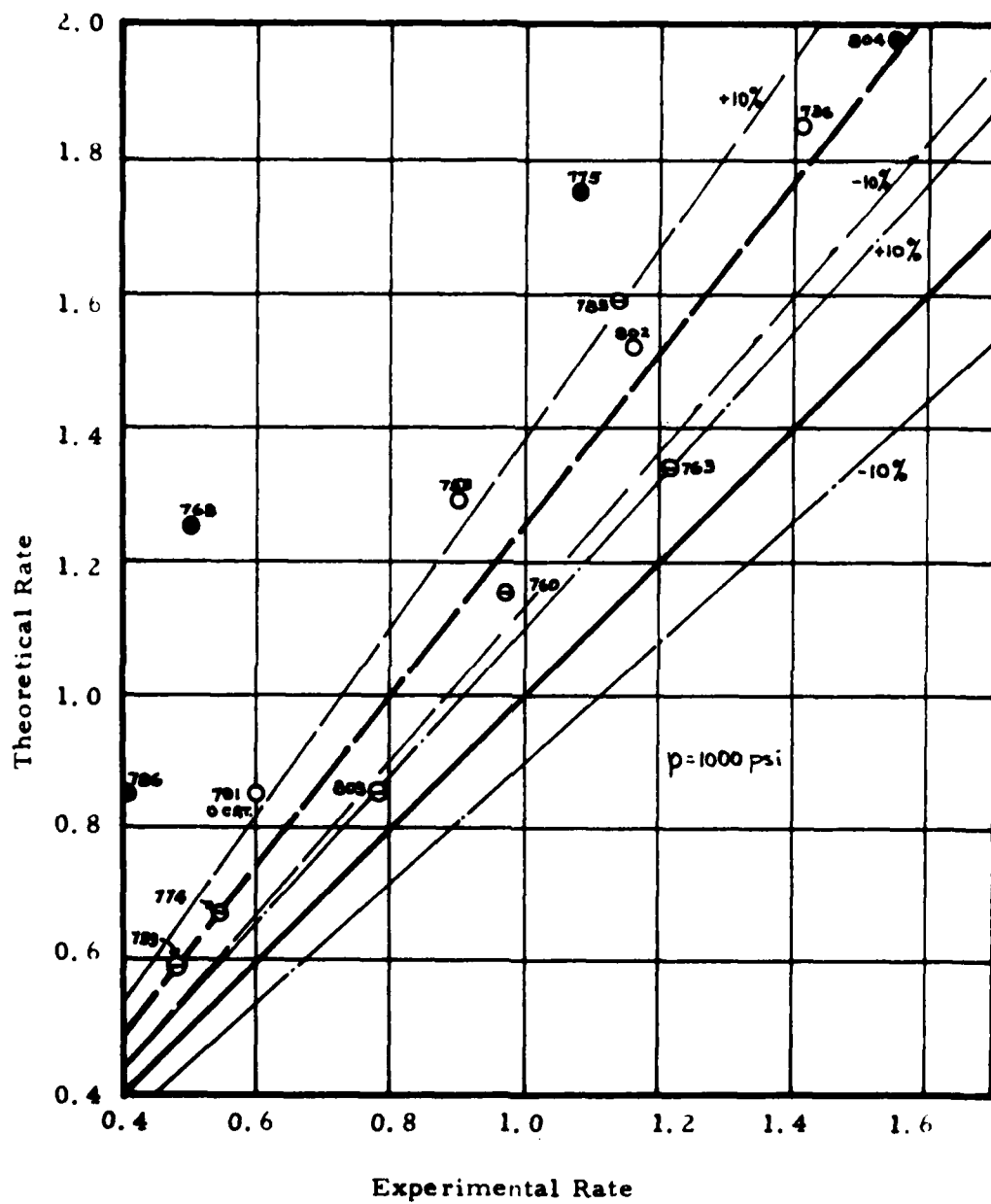


Figure 5. Burning Rate: Calculated versus Experimental for Maykut's Data Base

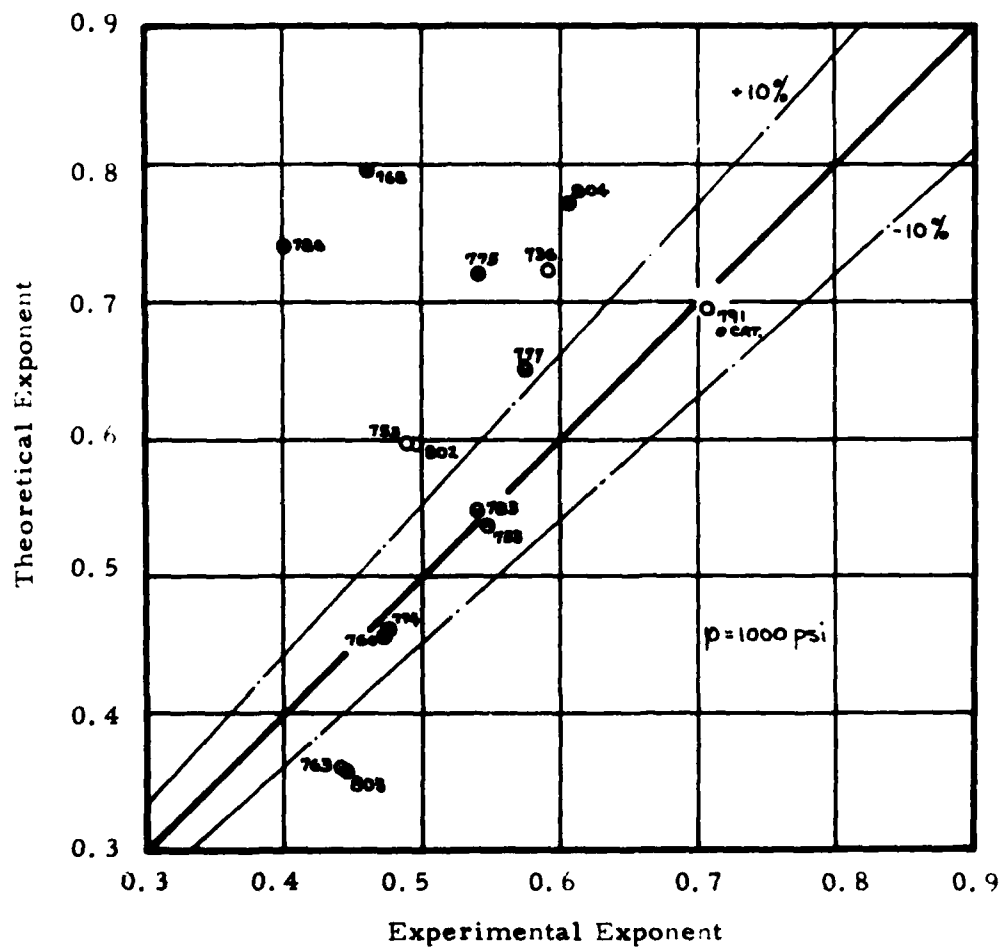


Figure 6. Burning Rate Exponent: Calculated versus Experimental for Maykut's Data Base

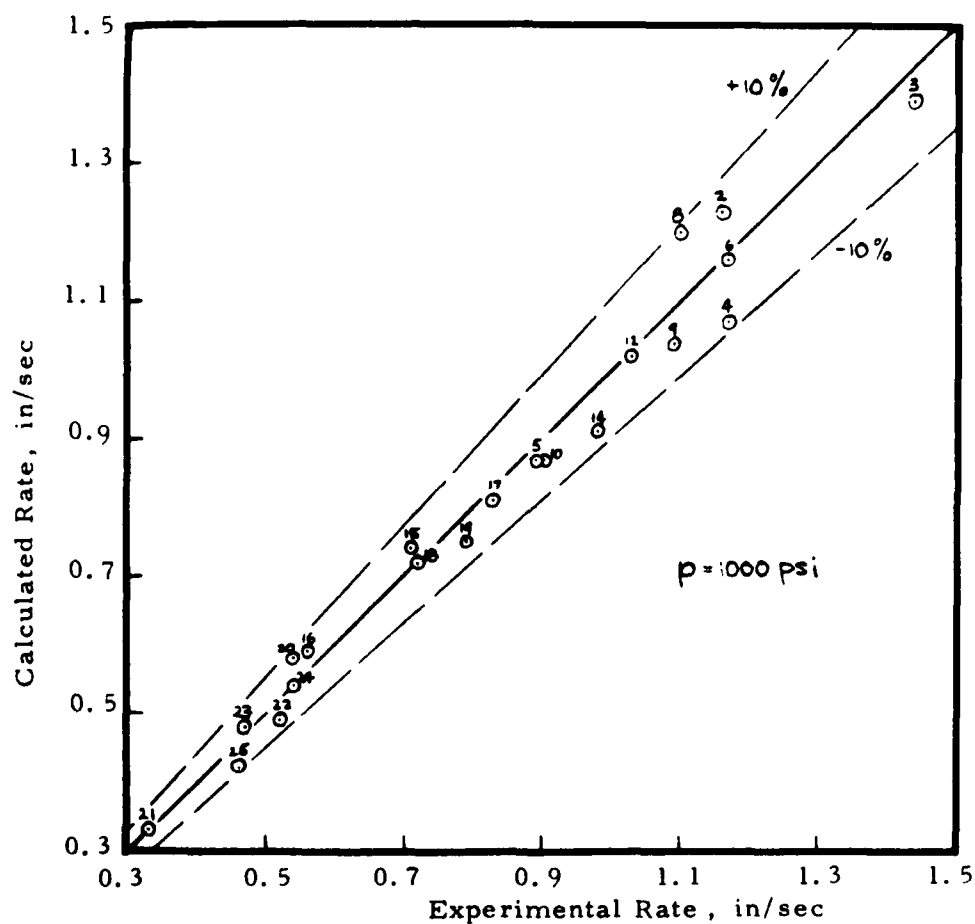


Figure 7. Burning Rate: Calculated versus Experimental for Miller's Additive Free Data Base (SD-III-88)



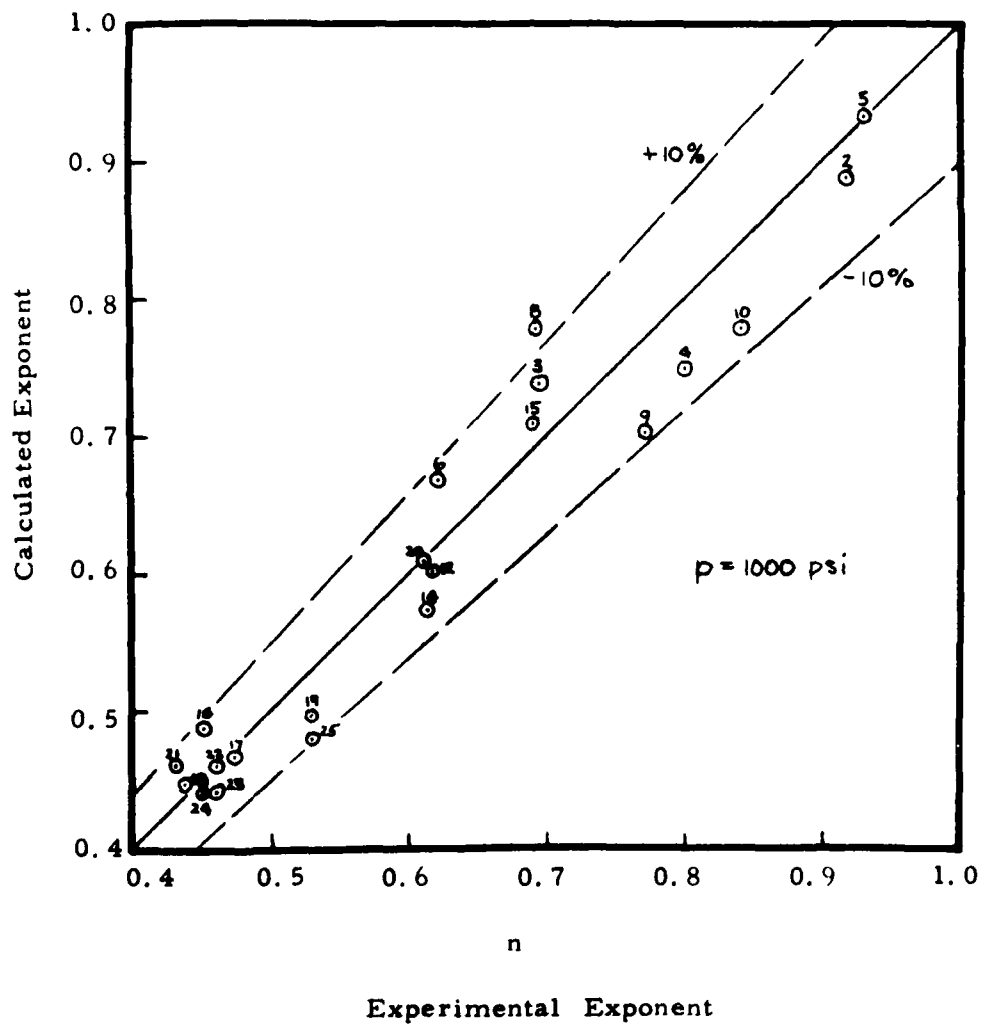


Figure 8. Exponent: Calculated Versus Experimental for Miller's Additive Free Data Base (SD-III-88)

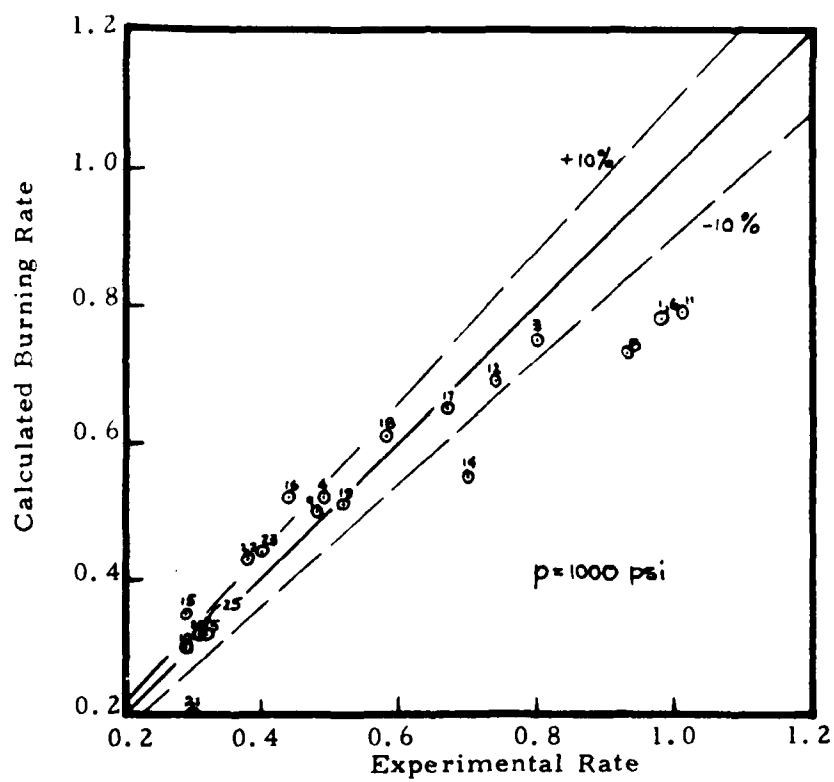


Figure 9. Burning Rate: Calculated versus Experimental for Miller's 18% 24-micron Aluminum Data Base (SD-I-88)

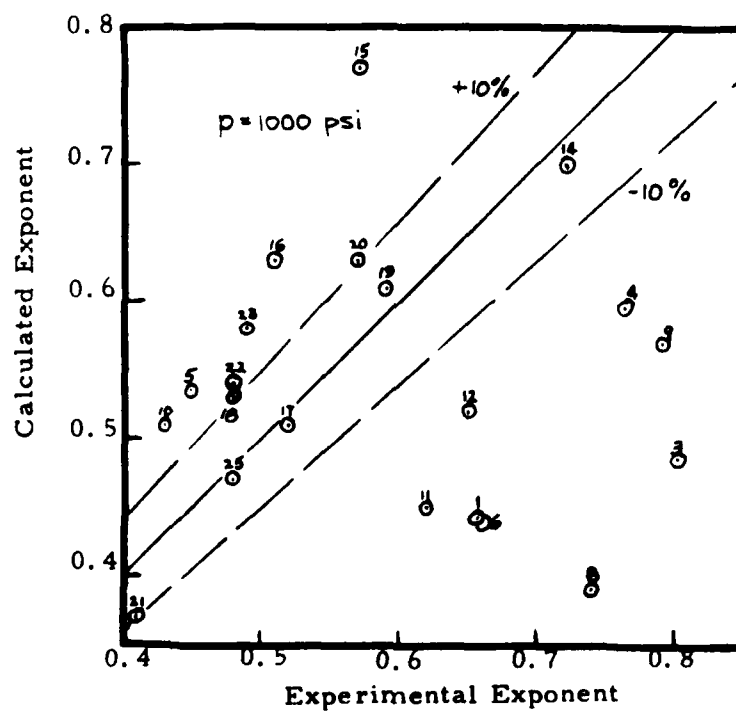


Figure 10. Burning Rate Exponent: Calculated versus Experimental for Miller's 24 micron Aluminum Additive Data Base (SD-I-88)

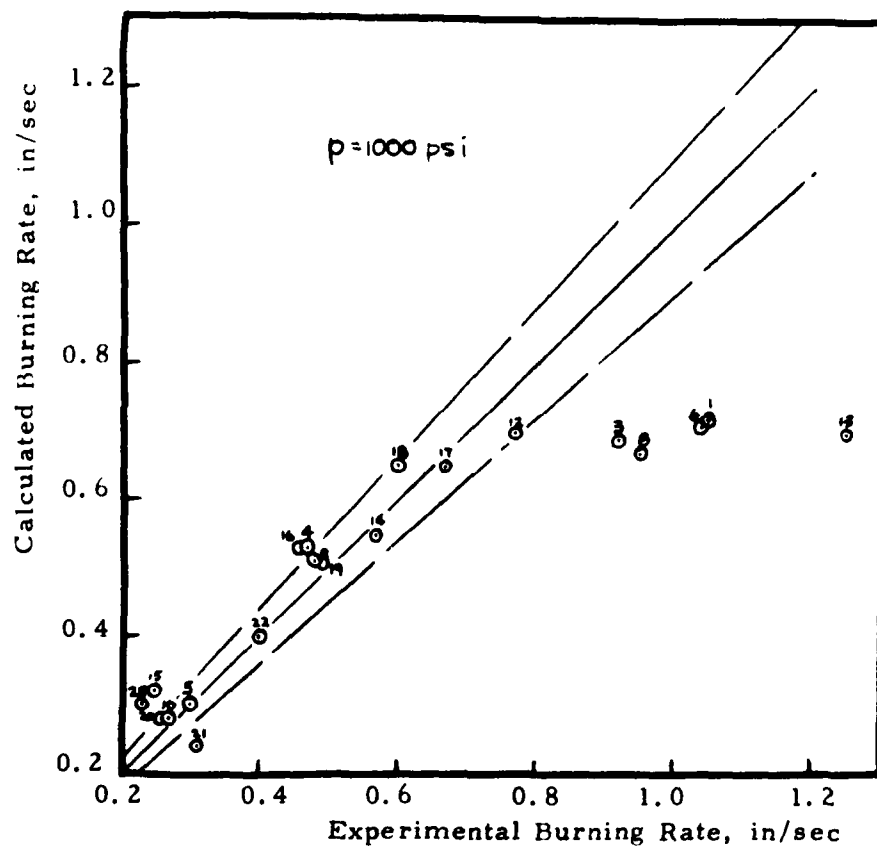


Figure 11. Burning Rate: Calculated versus Experimental for Miller's 90 micron Aluminum Additive Data Base (SD-IV-88)

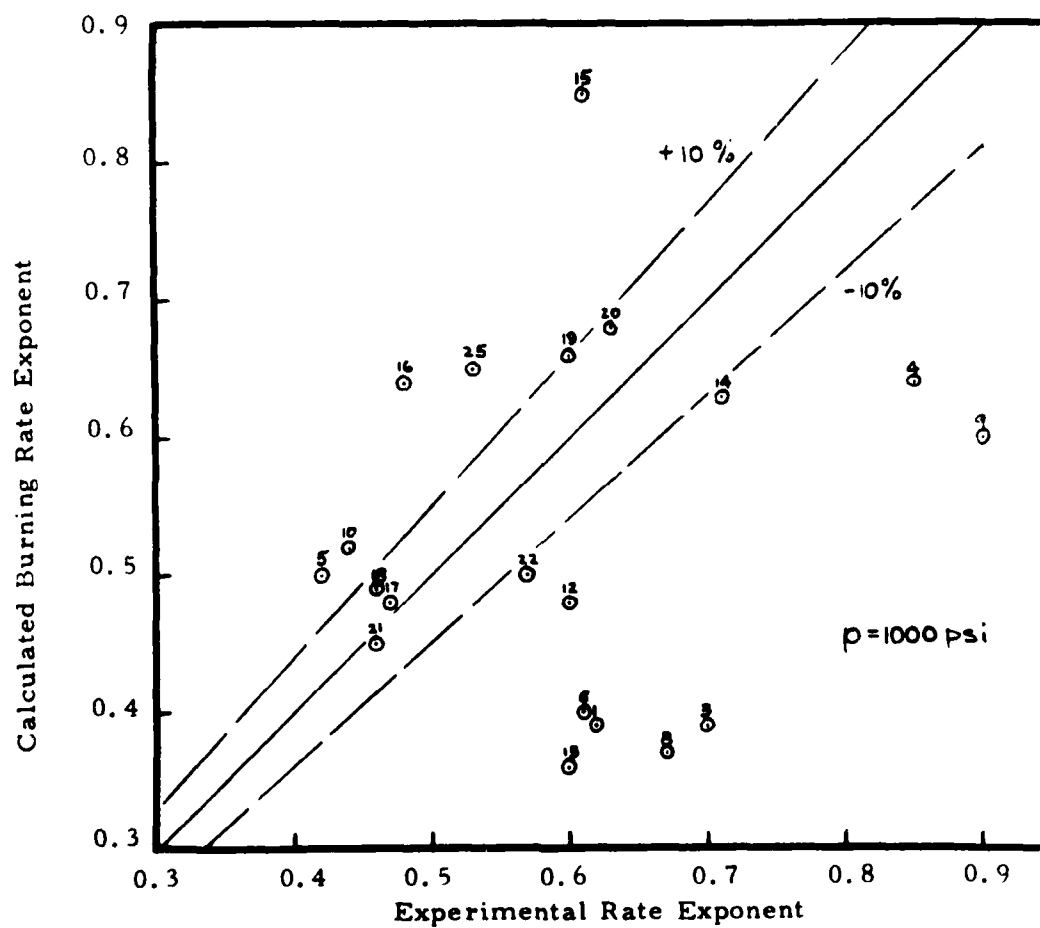


Figure 12. Burning Rate Exponent: Calculated versus Experimental for Miller's 90 micron Aluminum Additive Data Base (SD-IV-88)

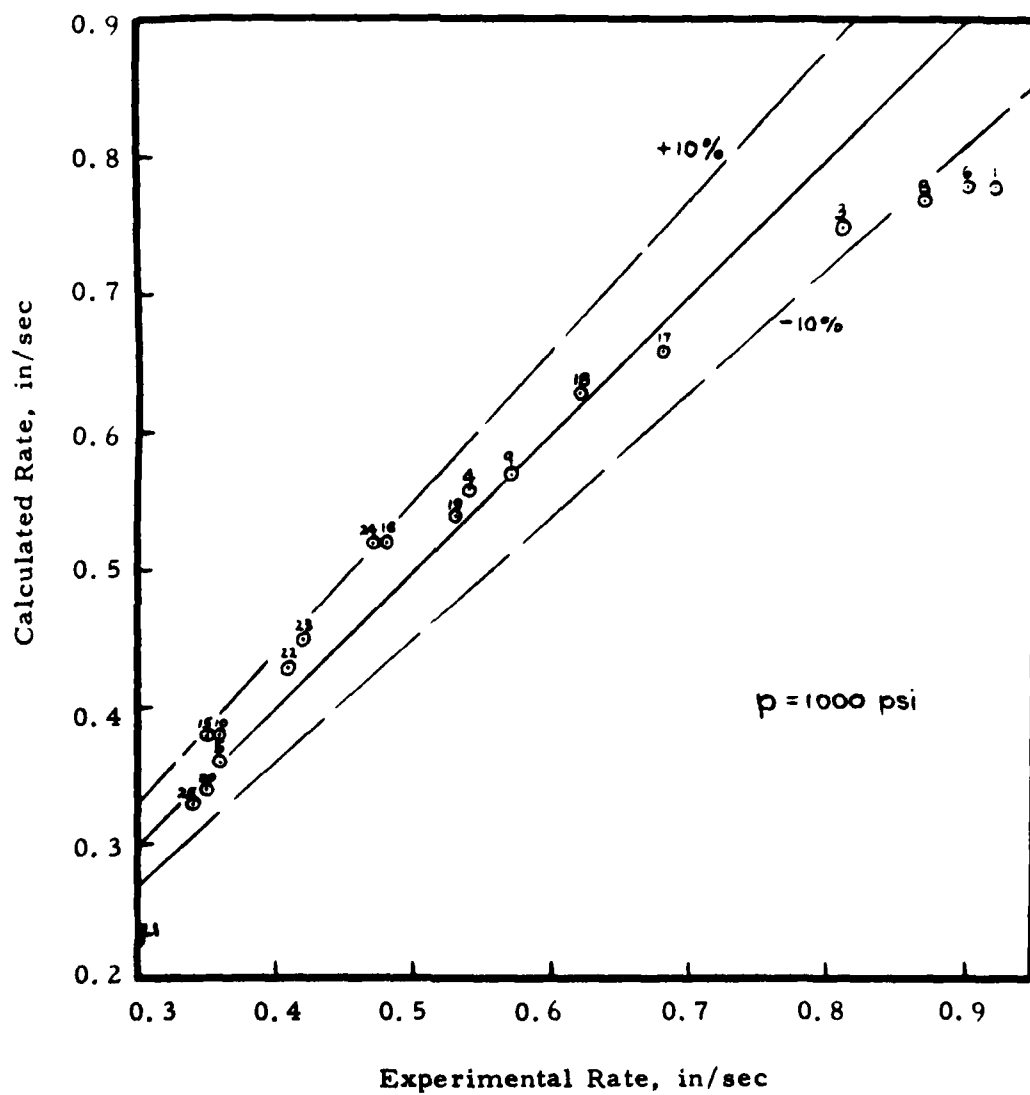


Figure 13. Burning Rate: Calculated Versus Experimental for Miller's  $6\mu$  Aluminum Data Base (SD-V-88)

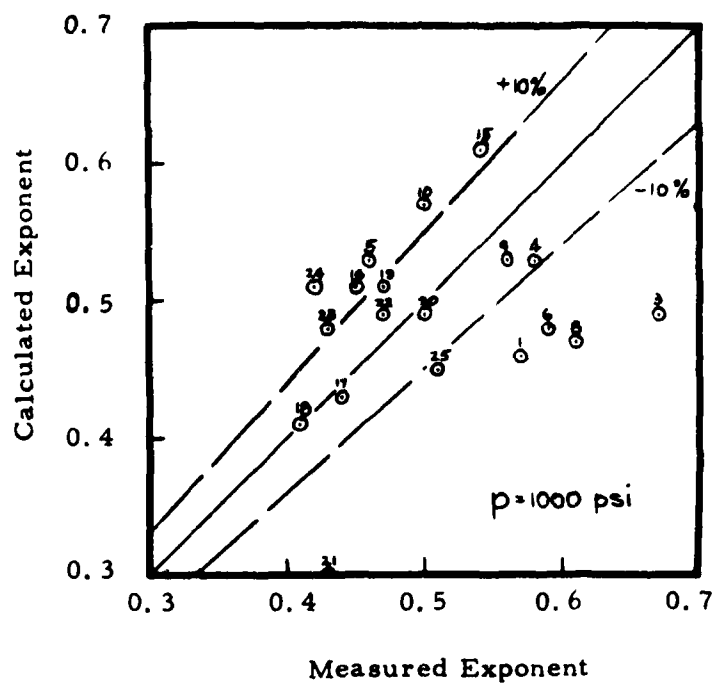


Figure 14. Exponent: Calculated Versus Experimental for Miller's 6 $\mu$  Aluminum Data Base (SD-V-88)

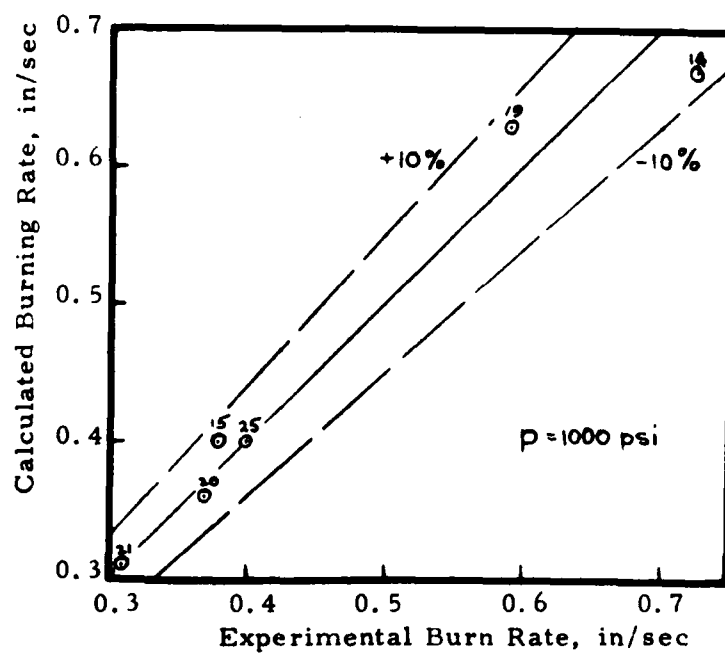


Figure 15. Burning Rate: Calculated versus Experimental for Miller's Extended Solids Data Base (SD-VI-90)



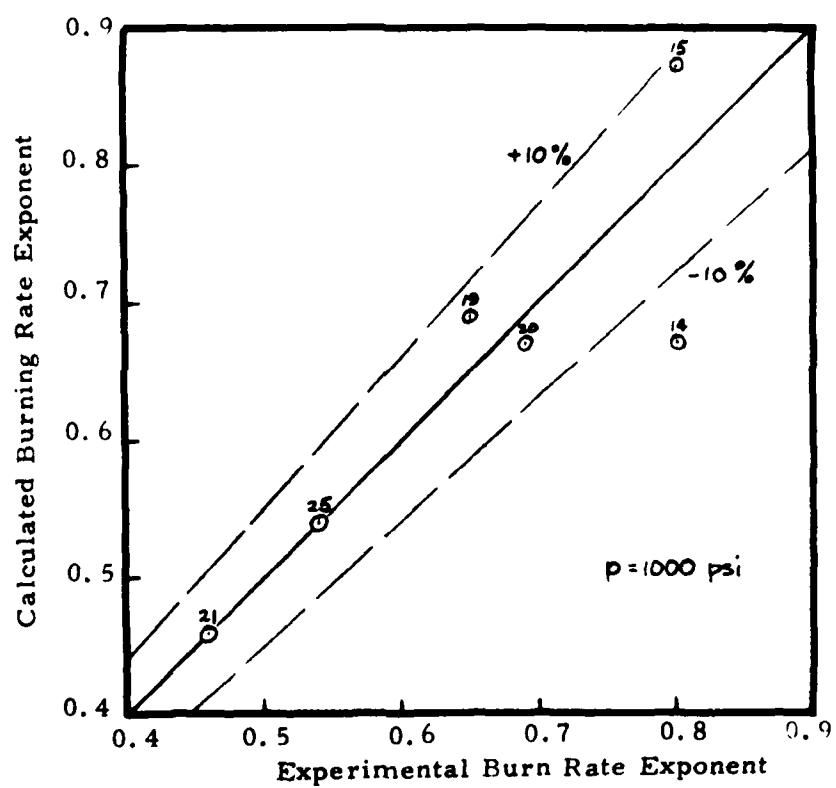


Figure 16. Burning Rate Exponent: Calculated versus Experimental for Miller's Extended Solids Data Base (SD-VI-90)

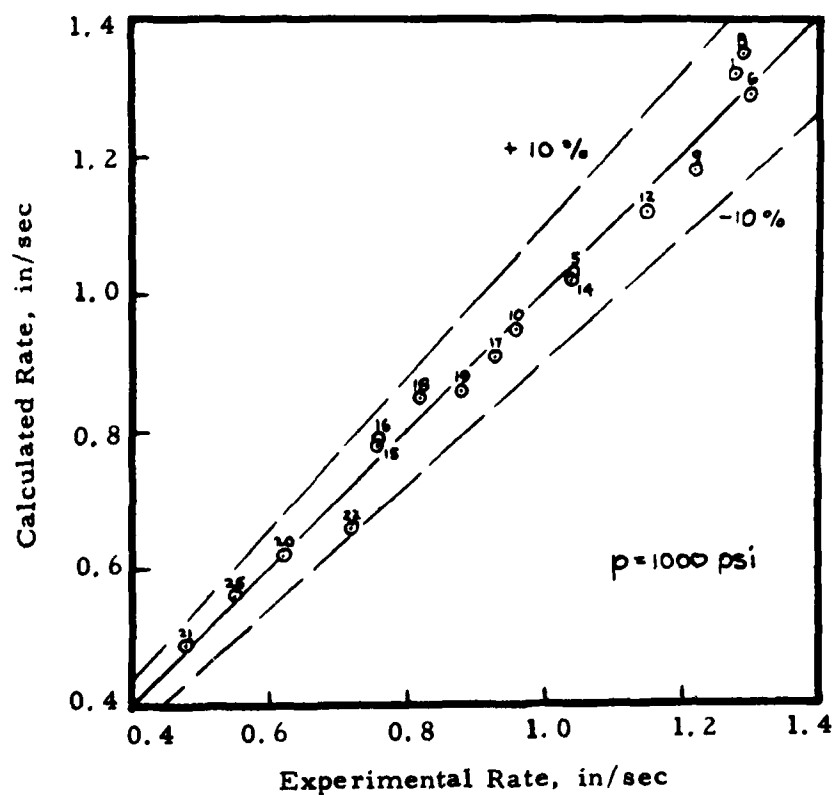


Figure 17. Burning Rate: Calculated Versus Experimental for Miller's 24 $\mu$  Aluminum/Iron Oxide Data Base (SD-VII-88)

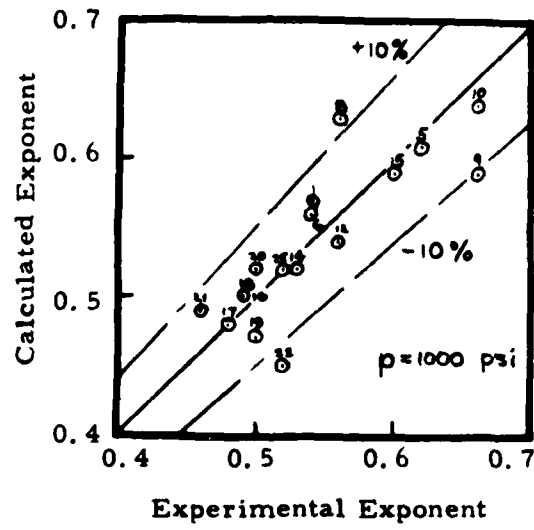


Figure 18. Exponent: Calculated Versus Experimental for Miller's 24 $\mu$  Aluminum/Iron Oxide Data Base (SD VII-88)

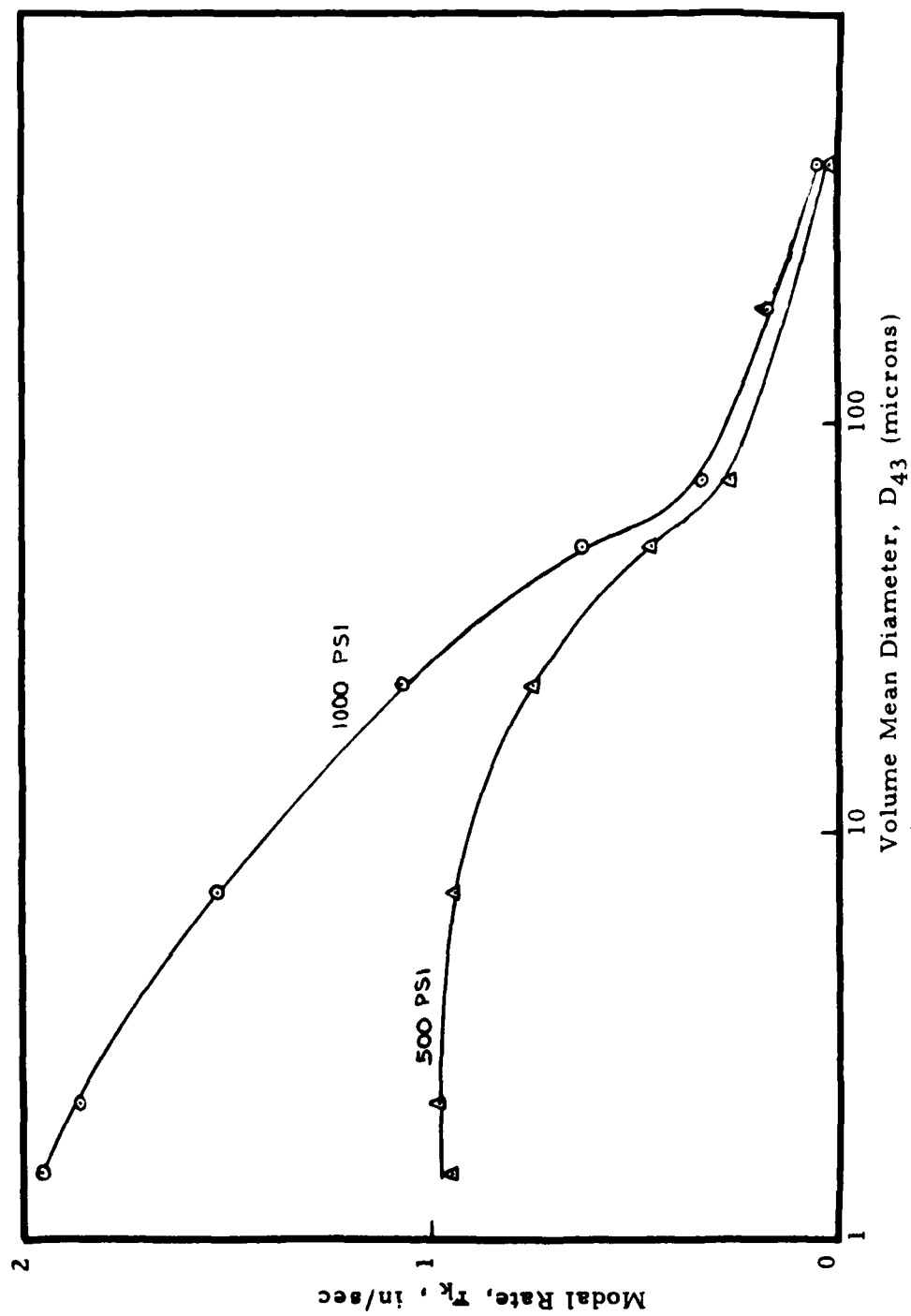


Figure 19. Variation of Modal Rates with Modal  $D_{43}$  (microns) for Miller's Additive Free Data Base (SD-III-88)

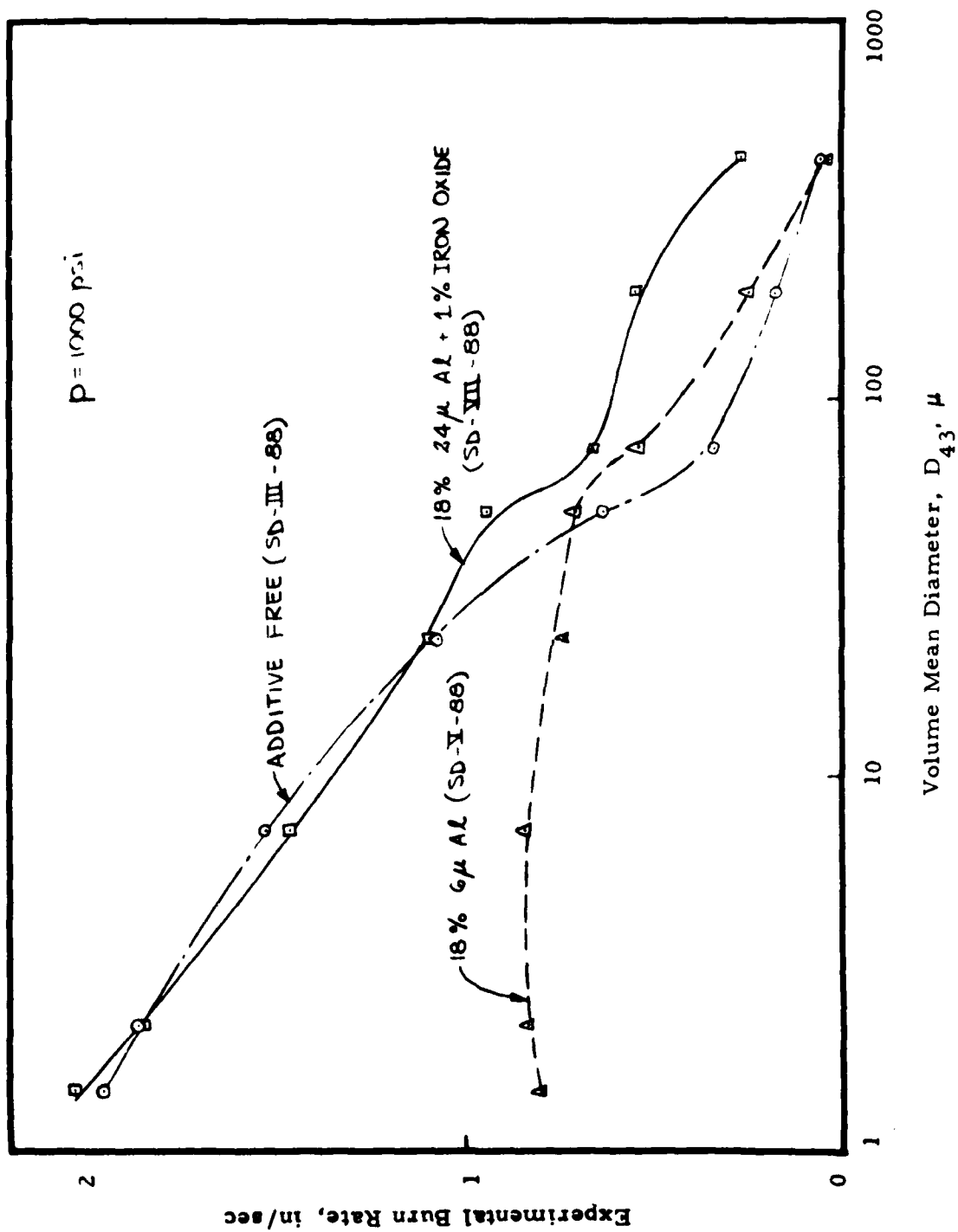


Figure 20. Effect of Volume Mean Diameter on Burn Rate, Miller's Data Base

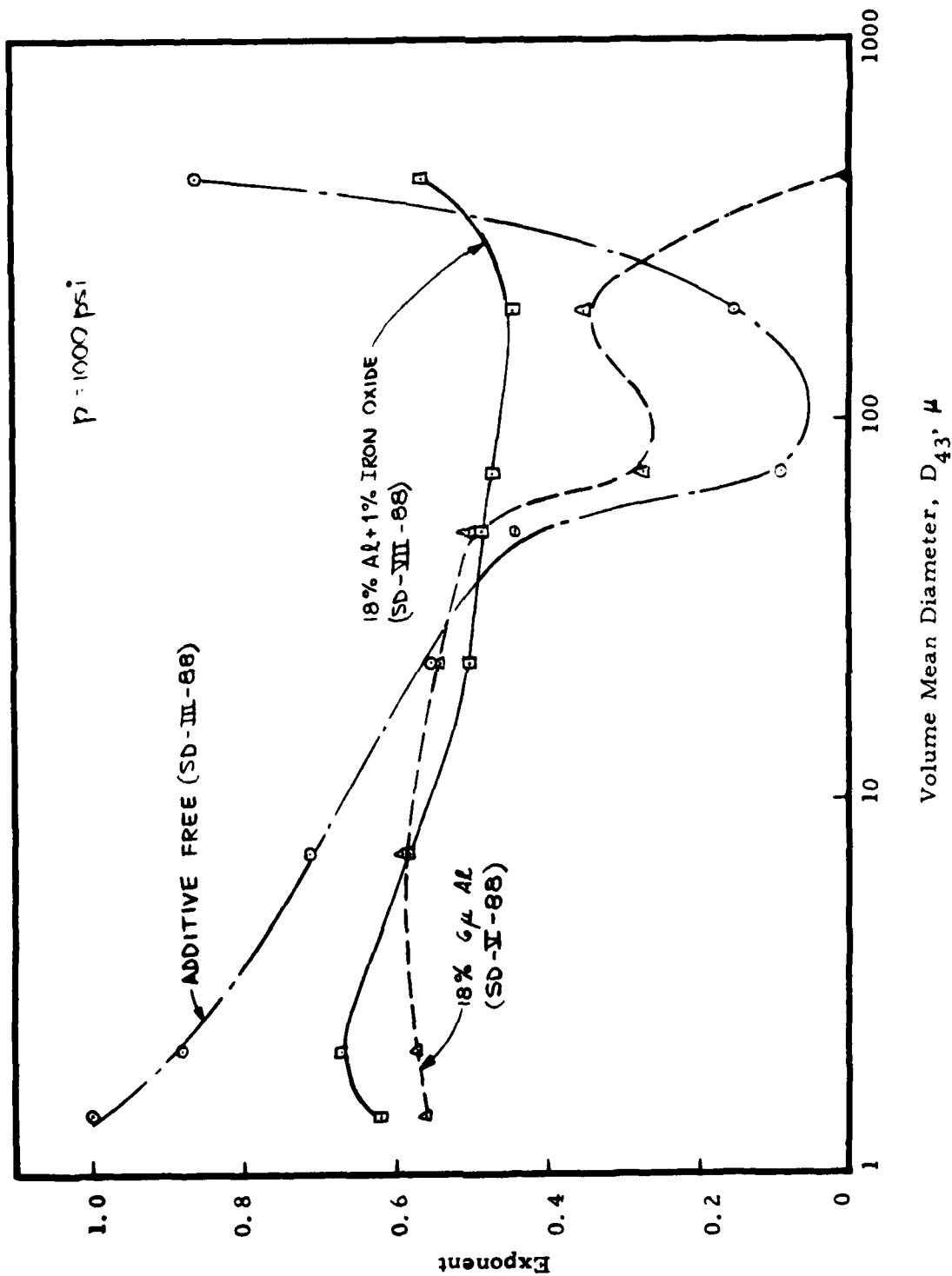


Figure 21. Effect of Volume Mean Diameter on Exponent, Miller's Data Base

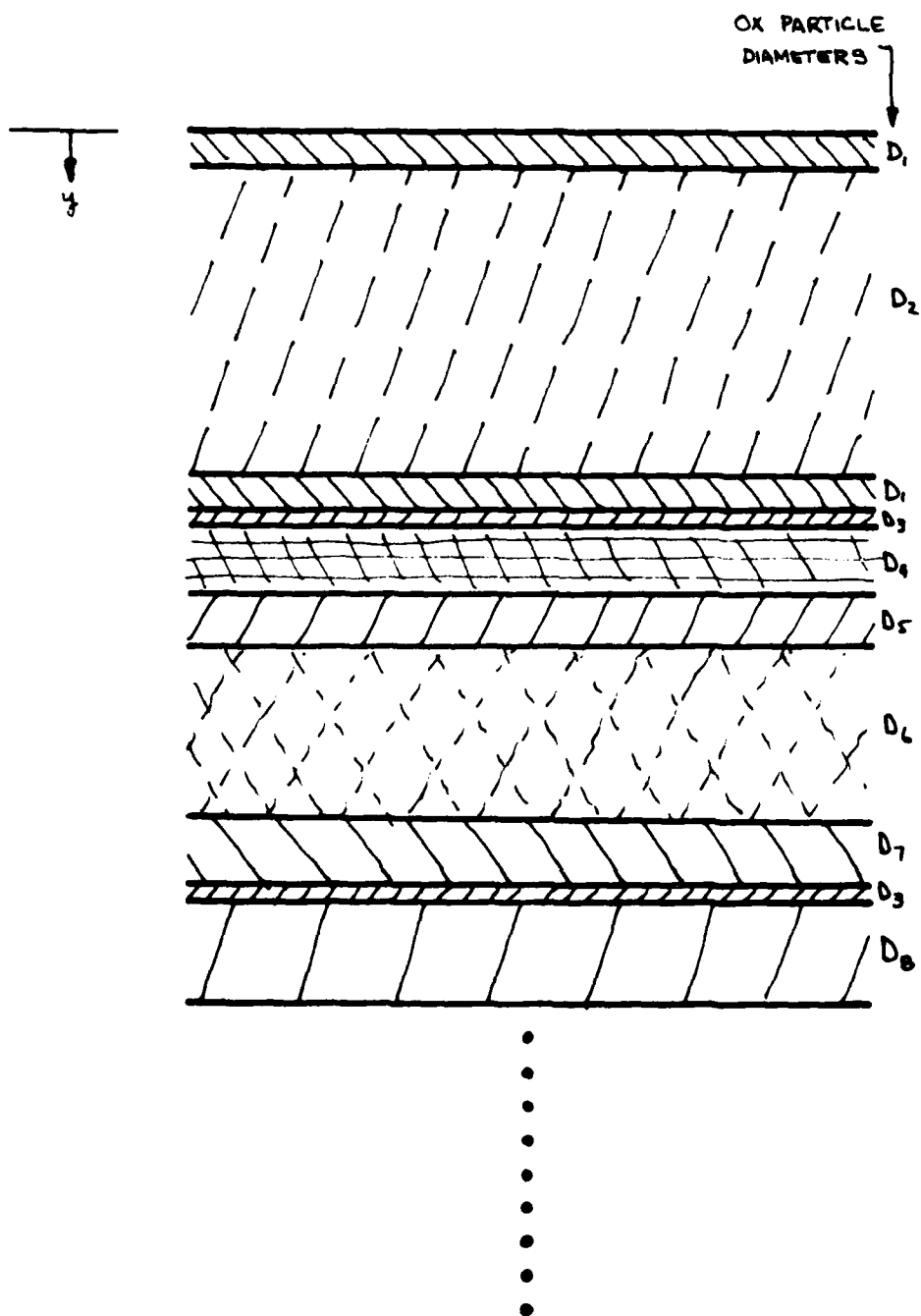


Figure 22. Schematic Illustrating Arrangement of Pseudopropellants

TABLE I

MODAL PROPERTIES FOR MILLER'S DATA BASE (1000 psi)

Formulation Designation	Modal Rates, in./sec.*									Modal Exponents†							Exponent SEE**	Comments	
	r <sub>400</sub>	r <sub>200</sub>	r <sub>90</sub>	r <sub>50</sub>	r <sub>20</sub>	r <sub>6</sub>	r <sub>2</sub>	r <sub>7</sub>	Rate SEE**	n <sub>400</sub>	n <sub>200</sub>	n <sub>90</sub>	n <sub>50</sub>	n <sub>20</sub>	n <sub>6</sub>	n <sub>2</sub>			n <sub>7</sub>
SD-III-88	.053	.190	.336	.628	1.074	1.517	1.859	1.949	.050	.859	.156	.088	.435	.553	.706	.878	.995	.092	Additive Free
SD-I-88	0.000	.215	.524	.748	.737	.823	.714	.750	.147	.492	.652	.377	.475	.612	.642	.484	.529	.217	18% 24μ Al
SD-IV-88	.000	.319	.643	.693	.648	.751	.661	.709	.203	.623	.650	.322	.506	.631	.657	.493	.495	.271	18% 90μ Al
SD-V-88	.044	.257	.541	.714	.744	.840	.826	.792	.090	.001	.353	.272	.492	.537	.590	.571	.555	.157	18% 60μ Al
SD-VII-88	.273	.546	.662	.943	1.090	1.459	1.852	2.032	.034	.563	.447	.473	.483	.498	.576	.670	.620	.058	18% 24μ Al 1% Iron Oxide
SD-VI-90	.029	.404	--	.900	.794	.890	--	--	.048	.000	.423	--	.563	.731	.868	--	--	.080	21% 24μ Al

\*Subscripts denote nominal diameter of mode in microns.

\*\*Standard Error of Estimate



TABLE II  
MODAL PROPERTIES FOR MAYKUT'S DATA BASE (1000 psi)

P psia	% Iron Oxide	Modal Rates, in/sec*			Modal Exponents*				Exponent SEE
		r <sub>200</sub>	r <sub>16</sub>	r <sub>1.7</sub>	Rate SEE**	n <sub>200</sub>	n <sub>16</sub>	n <sub>1.7</sub>	
700	0.5	0.000	0.907	1.273	.125				
700	0.75	0.021	0.839	1.665	.080				
700	2.0	0.137	1.050	1.611	.026				
1000	0.5	0.000	1.109	1.531	0.156	0.826	0.586	0.404	0.159
1000	0.75	0.000	.936	2.211	0.137	0.365	0.546	0.417	0.147
1000	2.0	0.179	1.215	2.158	0.020	0.331	0.433	0.593	0.018
2000	0.5	0.000	1.548	2.340	0.295				
2000	0.75	0.000	1.355	2.183	0.184				
2000	2.0	0.156	1.671	3.057	0.087				

\*Subscripts denote nominal diameter of mode in microns.

\*\*Standard Error of Estimate

APPENDIX A  
NOMENCLATURE

$D$	particle diameter
$E$	error
$F_{ox,k}$	distribution function for the $k$ th oxidizer mode
$m$	mass flux
$M$	number of oxidizer modes
$n$	pressure exponent
$N$	number of formulations
$p$	pressure
$q_s$	heat flux at the burning surface in the condensed phase
$r$	burning rate
$R_p$	pressure coupled response function
$t$	time
$T$	temperature
$y$	spatial coordinate
$\alpha$	oxidizer mass fraction
$\sigma_p$	temperature sensitivity at constant pressure

### Subscripts

D	denotes particles with $D \leq D < D + \Delta D$
j	denotes jth formulation
k	denotes kth oxidizer mode
n	denotes exponent
o	denotes initial conditions
ox	denotes oxidizer
r	denotes rate
s	denotes conditions at burning surface
t	denotes total propellant

### Special

( $\bar{\phantom{x}}$ )	bar over denotes a mean value
-------------------------	-------------------------------

## APPENDIX B MODAL PROPERTIES CODE

This computer program extracts modal properties from multi-modal propellant ballistic data according to the equations

$$\bar{r}_t = \sum_{k=1}^M \alpha_k \bar{r}_k / \alpha_t \quad \text{B-1}$$

$$\bar{n}_t = \sum_{k=1}^M \alpha_k \bar{r}_k \bar{n}_k / (\alpha_t \bar{r}_t) \quad \text{B-2}$$

where M is the number of oxidizer modes;  $\alpha_k$ ,  $\bar{r}_k$ ,  $\bar{n}_k$  are oxidizer mass fraction (mass ox/mass propellant), modal burn rate, and modal exponent respectively;  $\alpha_t$  is the total oxidizer content; and  $\bar{r}_t$  and  $\bar{n}_t$  are the measured burning rate and pressure exponent respectively.

A nonlinear optimizer (PATSH) is employed to extract the "best" modal parameters  $\bar{r}_k$ ,  $\bar{n}_k$   $k=1, M$  from a chemically consistent set of experimental data  $\bar{r}_{t,j}$ ,  $\alpha_{k,j}$ ,  $\bar{n}_{t,j}$   $j=1, N$  where  $N \geq M$ . A chemically consistent data set is one where all N formulations have the same chemical composition (variables are modal recipe and environment). The "best"  $\bar{r}_k$ ,  $\bar{n}_k$  is that which produces the smallest

$$E_r = \sqrt{\sum_{j=1}^N \left( \frac{\bar{r}_t - \bar{r}_{t,j}}{\bar{r}_{t,j}} \right)^2} / N$$

for the  $\bar{r}_k$  and the smallest

$$E_n = \sqrt{\sum_{j=1}^N \left( \frac{\bar{n}_t - \bar{n}_{t,j}}{\bar{n}_{t,j}} \right)^2} / N$$

for the  $\bar{n}_k$ .

Here  $\bar{r}_{t,j}$ ,  $\bar{n}_{t,j}$  refers to test data and  $\bar{r}_t$ ,  $\bar{n}_t$  to calculated (by Eqs. B.1 and B.2) results for the jth formulation. The "search" for the  $\bar{r}_k$  begins with  $\bar{r}_k = \bar{r}_{k+1} = \bar{r}_{t,1}$  and  $\bar{n}_k = \bar{n}_{k+1} = \bar{n}_{t,1}$ .

The input format consists of two major units. The first card defines the number of oxidizer modes, the number of formulations with these modes, the number of pressures at which data was obtained, and those pressures. Subsequent cards tabulate recipe, rate, and exponent for each formulation and pressure in the sequence. Figure B.1 illustrates a typical data set.

Output consists of the standard error of estimate of the fits and the  $r_k$ ,  $n_k$   $k=1, M$ . Figure B.2 illustrates results obtained from the Figure B.1 data set. Figure B.3 lists the Fortran IV code.

# MILLER DATA SET SD-III-1, -25 (ZERO ADDITIVE)

0821031000.500.2000.

.3158	.1368	.4211	.9161.165	.6272.214	-02
.5579	.5579	.3158	.6891.446	.3312.291	-03
.2421	.2421	.3158	.7971.168	.6321.909	-04
.1368	.1368	.3158	.929.970	.4711.704	-05
.3158.1368.3158.1057			.6211.160	.7371.744	-06
.3158.2421			.6921.096	.6801.774	-08
.2421			.7711.087	.6311.822	-09
.1368			.841.901	.5001.604	-10
.1368.4211			.6171.030	.6761.587	-12
.2421.3158			.613.978	.6371.490	-14
.1368.3158			.690.706	.4491.169	-15
.3158.2421			.451.561	.407.761	-16
.5579			.474.834	.6011.158	-17
.4526			.437.718	.521.955	-18
.5579			.527.785	.5361.116	-19
.4526			.610.539	.368.856	-20
.1053.1368			.430.330	.240.436	-21
.4211.1368			.458.524	.375.708	-22
.3158.1368			.463.469	.332.630	-23
.4211.1368			.449.536	.393.732	-24
.3158.1368			.528.445	.304.652	-25

Figure B.1 - Input Format for Code

WILLER DATA SET SD-III-1-25 (ZERO ADJUSTED)

FX MASS FUNCTION DATA												EXPERIMENTAL DATA				
MODE 1	MODE 2	MODE 3	MODE 4	MODE 5	MODE 6	MODE 7	MODE 8	A(01)	A(02)	A(03)	A(04)	A(05)				
0.0	0.0	0.3158	0.0	0.1368	0.0	0.0	0.0	0.0	0.0	0.0	0.0	0.0				
0.0	0.0	0.0	0.0	0.5575	0.0	0.0	0.0	0.0	0.0	0.0	0.0	0.0				
0.0	0.3158	0.0	0.0	0.2421	0.0	0.0	0.0	0.0	0.0	0.0	0.0	0.0				
0.4211	0.0	0.0	0.0	0.1368	0.0	0.0	0.0	0.0	0.0	0.0	0.0	0.0				
0.0	0.0	0.0	0.3158	0.1368	0.0	0.0	0.0	0.0	0.0	0.0	0.0	0.0				
0.0	0.0	0.0	0.3158	0.2421	0.0	0.0	0.0	0.0	0.0	0.0	0.0	0.0				
0.0	0.3158	0.0	0.0	0.2421	0.0	0.0	0.0	0.0	0.0	0.0	0.0	0.0				
0.0	0.0	0.0	0.0	0.1368	0.0	0.0	0.0	0.0	0.0	0.0	0.0	0.0				
0.4211	0.0	0.0	0.0	0.1368	0.0	0.0	0.0	0.0	0.0	0.0	0.0	0.0				
0.0	0.0	0.3158	0.0	0.1368	0.0	0.0	0.0	0.0	0.0	0.0	0.0	0.0				
0.0	0.3158	0.0	0.0	0.2421	0.0	0.0	0.0	0.0	0.0	0.0	0.0	0.0				
0.0	0.0	0.0	0.0	0.1368	0.0	0.0	0.0	0.0	0.0	0.0	0.0	0.0				
0.4211	0.0	0.0	0.0	0.1368	0.0	0.0	0.0	0.0	0.0	0.0	0.0	0.0				
0.0	0.0	0.0	0.0	0.5575	0.0	0.0	0.0	0.0	0.0	0.0	0.0	0.0				
0.0	0.0	0.3158	0.0	0.5575	0.0	0.0	0.0	0.0	0.0	0.0	0.0	0.0				
0.0	0.0	0.0	0.4211	0.5575	0.0	0.0	0.0	0.0	0.0	0.0	0.0	0.0				
0.0	0.3158	0.0	0.0	0.5575	0.0	0.0	0.0	0.0	0.0	0.0	0.0	0.0				
0.0	0.0	0.0	0.0	0.4526	0.0	0.0	0.0	0.0	0.0	0.0	0.0	0.0				
0.0	0.3158	0.0	0.0	0.5575	0.0	0.0	0.0	0.0	0.0	0.0	0.0	0.0				
0.4211	0.0	0.0	0.0	0.4526	0.0	0.0	0.0	0.0	0.0	0.0	0.0	0.0				
0.3158	0.3158	0.0	0.1053	0.1368	0.0	0.0	0.0	0.0	0.0	0.0	0.0	0.0				
0.3158	0.0	0.0	0.4211	0.1368	0.0	0.0	0.0	0.0	0.0	0.0	0.0	0.0				
0.0	0.4211	0.0	0.3158	0.1368	0.0	0.0	0.0	0.0	0.0	0.0	0.0	0.0				
0.0	0.3158	0.0	0.4211	0.1368	0.0	0.0	0.0	0.0	0.0	0.0	0.0	0.0				
0.4211	0.0	0.0	0.3158	0.1368	0.0	0.0	0.0	0.0	0.0	0.0	0.0	0.0				

Figure B.2 - Sample Output

MILLER DATA SET 50-111-1-25 (ZERO ADDITIVE)

P = 1000.0 PSI RATE STD ERR = 4.9802E-02 EXPONENT STD ERR = 6.1590E-02

COMPUTED NUCAL RATES, IN/SEC

RM1 RM2 RM3 RM4 RM5 RM6 RM7 RM8 RM9 RM10 RM11 RM12 RM13 RM14 RM15 RM16 RM17 RM18 RM19 RM20

-0.0325 0.1896 0.3358 0.6277 1.0735 1.5172 1.8594 1.9486 0.8593 0.1526 -0.0884 0.4352 0.5526 1.7056 0.8743 0.9950

COMPARISON THEORY/EXPERIMENT

R	RC	ERR	N	NC	ERN
1.1650	1.2268	-0.0530	0.9160	0.8879	0.0207
1.4460	1.3884	0.0398	0.6890	0.7447	-0.0558
1.1680	1.0690	0.0848	0.7970	0.7473	0.0523
0.8700	0.8963	-0.0303	0.9280	0.9361	-0.0066
1.1600	1.1674	-0.0064	0.6210	0.6695	-0.0485
1.0960	1.1964	-0.0916	0.6920	0.7787	-0.0867
1.0470	1.0381	0.0089	0.7710	0.7039	0.0670
0.9910	0.8654	0.0355	0.8410	0.7824	0.0586
1.0300	1.0207	0.0093	0.6170	0.6016	0.0154
0.9780	0.9144	0.0650	0.6130	0.5744	0.0386
0.7040	0.7418	-0.0378	0.6900	0.7105	-0.0197
0.5610	0.5929	-0.0319	0.4510	0.4876	-0.0366
0.8340	0.8049	0.0291	0.4740	0.4671	0.0069
0.7180	0.7180	0.0001	0.4370	0.4479	-0.0109
0.7850	0.7540	0.0310	0.5290	0.4559	0.0731
0.5390	0.5814	-0.0424	0.6100	0.6105	-0.0005
0.3300	0.3312	-0.0012	0.4300	0.4623	-0.0323
0.5240	0.4896	0.0344	0.4580	0.4596	-0.0016
0.4690	0.4664	-0.0024	0.4630	0.4383	0.0247
0.5360	0.5391	-0.0031	0.4490	0.4384	0.0106
0.4450	0.4203	0.0247	0.5280	0.4794	0.0486

Figure B.2 - Sample Output (continued)



MILLER DATA SET 50-111-1.-25 (ZERO ADDITIVE)

P = 300.0 PSI RATE STD ERR= 4.7113E-02 EXPONENT STD ERR= 6.1590E-02

COMPUTED WTCAL RATES, IN/SEC

NAME

NAME

NAME

NAME

NAME

NAME

NAME

NAME

NAME

NAME

NAME

NAME

NAME

NAME

NAME

NAME

NAME

-0.0276 0.1434 0.2674 0.4581 0.749C 0.9413 0.9800 C.9468

COMPARISON THEORY/EXPERIMENT

EPA

NC

N

ERR

RC

R

C.6270 0.6705 -0.6694  
 0.8010 0.8207 0.8685  
 0.6320 0.6018 0.0478  
 0.4710 0.4730 -0.0042  
 0.7370 0.7412 -0.0057  
 0.6800 0.7274 -0.0496  
 0.6310 0.6134 0.0276  
 0.5000 0.4848 0.0304  
 0.6760 0.6676 0.0124  
 0.6370 0.5996 0.0587  
 0.4490 0.4708 -0.0486  
 0.4070 0.4249 -0.0441  
 0.6010 0.5749 0.0434  
 0.5210 0.5169 0.0079  
 0.5340 0.5301 0.111C  
 0.3680 0.4013 -0.0904  
 0.2400 0.2343 0.0239  
 0.3790 0.3480 0.0719  
 0.3320 0.3520 -0.0601  
 0.3930 0.3899 0.0079  
 0.3040 0.2961 0.0258

Figure B. 2- Sample Output (continued)

# MILLER DATA SET SD-111-1.-25 (ZERO ADDITIVE)

P = 2000.0 PSI RATE STD ERR = 4.4083E-02 EXPONENT STD ERR = 5.1590E-02

COMPUTER TOTAL RATES, IN/SEC

COMPUTER TOTAL RATES, IN/SEC

COMPARISON THEORY/EXPERIMENT

COMPARISON THEORY/EXPERIMENT

COMPUTER TOTAL RATES, IN/SEC

Figure B.2 - Sample Output (concluded)



```

00000590
00000600
00000610
00000620
00000630
00000640
00000650
00000660
00000670
00000680
00000690
00000700
00000710
00000720
00000730
00000740
00000750
00000760
00000770
00000780
00000790
00000800
00000810
00000820
00000830
00000840
00000850
00000860
00000870
00000880
00000890
00000900
00000910
00000920
00000930
00000940
00000950
00000960
00000970
00000980
00000990
00010000
00010010
00010020
00010030
00010040
00010050
00010060
00010070
00010080
00010090
00010100
00010110
00010120
00010130
00010140
00010150
00010160

C COMPUTE ALFAT(I,J)
C
  DO 67 J=1,JJ
    ALFAT(I,J)=0.0
    DO 63 I=1,II
      ALFAT(I,J)=4*FAT(J)*ALFAT(I,J)
      CONTINUE
    67 CONTINUE
  C
  C FIND NM(I,K) FOR EACH P(K)
  C
    DO 200 M=1,MX
      C SET INITIAL NM(I,K)
      C
        DO 70 I=1,II
          NM(I)=NM(I,K)
          IF(K.EQ.1) NM(I)=P(I)
          CONTINUE
        70 CONTINUE
      C
      C FIND OPTIMAL NM(I,K)
      C
        80 CALL PATSH(QMA,FRR1,II,5.0,CJOL,50,-1,MQNEP1)
        DO 90 I=1,II
          NM(I,K)=NM(I)
        90 NM(I,K)=NM(I)
      C
      C NEED FIND NM(II) ?
      C
        IF(K.GT.1) KPRINT=2
        IF(N(1).EQ.0.0) KPRINT=2
        IF(KPRINT.EQ.2) GO TO 100
      C
      C FIND OPTIMAL N(II)
      C
        CALL PATSH(NM,EPR2,II,5.0,0.0J1,50,-1,MQNEP4)
      C
      C OUTPUT COMPUTED RESULTS THIS P(K)
      C
        100 WRITE(6,110) MEAC
        110 FORMAT(1H,20A4)
        115 FCPRAT(1H),3HP =56,1,44 DS1,5X,'RATE STD ERR=' ,1PE11,4,5X,'EXPINE 7001,700'
        INT STD ERR=' ,1PE11,4,77ZH 4,16X,'COMPUTED MODAL EXPONENTS',21X,IM0,77ZH 4,16X,'RM1',5X,'RM2',5X,'RM3',5X,'RM4',5X,'RM5',5X,'RM6',5X,'RM7',5X,'RM8',5X,'RM9',5X,'RM10',5X,'RM11',5X,'RM12',5X,'RM13',5X,'RM14',5X,'RM15',5X,'RM16',5X,'RM17',5X,'RM18',5X,'RM19',5X,'RM20',5X,'RM21',5X,'RM22',5X,'RM23',5X,'RM24',5X,'RM25',5X,'RM26',5X,'RM27',5X,'RM28',5X,'RM29',5X,'RM30',5X,'RM31',5X,'RM32',5X,'RM33',5X,'RM34',5X,'RM35',5X,'RM36',5X,'RM37',5X,'RM38',5X,'RM39',5X,'RM40',5X,'RM41',5X,'RM42',5X,'RM43',5X,'RM44',5X,'RM45',5X,'RM46',5X,'RM47',5X,'RM48',5X,'RM49',5X,'RM50',5X,'RM51',5X,'RM52',5X,'RM53',5X,'RM54',5X,'RM55',5X,'RM56',5X,'RM57',5X,'RM58',5X,'RM59',5X,'RM60',5X,'RM61',5X,'RM62',5X,'RM63',5X,'RM64',5X,'RM65',5X,'RM66',5X,'RM67',5X,'RM68',5X,'RM69',5X,'RM70',5X,'RM71',5X,'RM72',5X,'RM73',5X,'RM74',5X,'RM75',5X,'RM76',5X,'RM77',5X,'RM78',5X,'RM79',5X,'RM80',5X,'RM81',5X,'RM82',5X,'RM83',5X,'RM84',5X,'RM85',5X,'RM86',5X,'RM87',5X,'RM88',5X,'RM89',5X,'RM90',5X,'RM91',5X,'RM92',5X,'RM93',5X,'RM94',5X,'RM95',5X,'RM96',5X,'RM97',5X,'RM98',5X,'RM99',5X,'RM100',5X,'RM101',5X,'RM102',5X,'RM103',5X,'RM104',5X,'RM105',5X,'RM106',5X,'RM107',5X,'RM108',5X,'RM109',5X,'RM110',5X,'RM111',5X,'RM112',5X,'RM113',5X,'RM114',5X,'RM115',5X,'RM116',5X,'RM117',5X,'RM118',5X,'RM119',5X,'RM120',5X,'RM121',5X,'RM122',5X,'RM123',5X,'RM124',5X,'RM125',5X,'RM126',5X,'RM127',5X,'RM128',5X,'RM129',5X,'RM130',5X,'RM131',5X,'RM132',5X,'RM133',5X,'RM134',5X,'RM135',5X,'RM136',5X,'RM137',5X,'RM138',5X,'RM139',5X,'RM140',5X,'RM141',5X,'RM142',5X,'RM143',5X,'RM144',5X,'RM145',5X,'RM146',5X,'RM147',5X,'RM148',5X,'RM149',5X,'RM150',5X,'RM151',5X,'RM152',5X,'RM153',5X,'RM154',5X,'RM155',5X,'RM156',5X,'RM157',5X,'RM158',5X,'RM159',5X,'RM160',5X,'RM161',5X,'RM162',5X,'RM163',5X,'RM164',5X,'RM165',5X,'RM166',5X,'RM167',5X,'RM168',5X,'RM169',5X,'RM170',5X,'RM171',5X,'RM172',5X,'RM173',5X,'RM174',5X,'RM175',5X,'RM176',5X,'RM177',5X,'RM178',5X,'RM179',5X,'RM180',5X,'RM181',5X,'RM182',5X,'RM183',5X,'RM184',5X,'RM185',5X,'RM186',5X,'RM187',5X,'RM188',5X,'RM189',5X,'RM190',5X,'RM191',5X,'RM192',5X,'RM193',5X,'RM194',5X,'RM195',5X,'RM196',5X,'RM197',5X,'RM198',5X,'RM199',5X,'RM200',5X,'RM201',5X,'RM202',5X,'RM203',5X,'RM204',5X,'RM205',5X,'RM206',5X,'RM207',5X,'RM208',5X,'RM209',5X,'RM210',5X,'RM211',5X,'RM212',5X,'RM213',5X,'RM214',5X,'RM215',5X,'RM216',5X,'RM217',5X,'RM218',5X,'RM219',5X,'RM220',5X,'RM221',5X,'RM222',5X,'RM223',5X,'RM224',5X,'RM225',5X,'RM226',5X,'RM227',5X,'RM228',5X,'RM229',5X,'RM230',5X,'RM231',5X,'RM232',5X,'RM233',5X,'RM234',5X,'RM235',5X,'RM236',5X,'RM237',5X,'RM238',5X,'RM239',5X,'RM240',5X,'RM241',5X,'RM242',5X,'RM243',5X,'RM244',5X,'RM245',5X,'RM246',5X,'RM247',5X,'RM248',5X,'RM249',5X,'RM250',5X,'RM251',5X,'RM252',5X,'RM253',5X,'RM254',5X,'RM255',5X,'RM256',5X,'RM257',5X,'RM258',5X,'RM259',5X,'RM260',5X,'RM261',5X,'RM262',5X,'RM263',5X,'RM264',5X,'RM265',5X,'RM266',5X,'RM267',5X,'RM268',5X,'RM269',5X,'RM270',5X,'RM271',5X,'RM272',5X,'RM273',5X,'RM274',5X,'RM275',5X,'RM276',5X,'RM277',5X,'RM278',5X,'RM279',5X,'RM280',5X,'RM281',5X,'RM282',5X,'RM283',5X,'RM284',5X,'RM285',5X,'RM286',5X,'RM287',5X,'RM288',5X,'RM289',5X,'RM290',5X,'RM291',5X,'RM292',5X,'RM293',5X,'RM294',5X,'RM295',5X,'RM296',5X,'RM297',5X,'RM298',5X,'RM299',5X,'RM300',5X,'RM301',5X,'RM302',5X,'RM303',5X,'RM304',5X,'RM305',5X,'RM306',5X,'RM307',5X,'RM308',5X,'RM309',5X,'RM310',5X,'RM311',5X,'RM312',5X,'RM313',5X,'RM314',5X,'RM315',5X,'RM316',5X,'RM317',5X,'RM318',5X,'RM319',5X,'RM320',5X,'RM321',5X,'RM322',5X,'RM323',5X,'RM324',5X,'RM325',5X,'RM326',5X,'RM327',5X,'RM328',5X,'RM329',5X,'RM330',5X,'RM331',5X,'RM332',5X,'RM333',5X,'RM334',5X,'RM335',5X,'RM336',5X,'RM337',5X,'RM338',5X,'RM339',5X,'RM340',5X,'RM341',5X,'RM342',5X,'RM343',5X,'RM344',5X,'RM345',5X,'RM346',5X,'RM347',5X,'RM348',5X,'RM349',5X,'RM350',5X,'RM351',5X,'RM352',5X,'RM353',5X,'RM354',5X,'RM355',5X,'RM356',5X,'RM357',5X,'RM358',5X,'RM359',5X,'RM360',5X,'RM361',5X,'RM362',5X,'RM363',5X,'RM364',5X,'RM365',5X,'RM366',5X,'RM367',5X,'RM368',5X,'RM369',5X,'RM370',5X,'RM371',5X,'RM372',5X,'RM373',5X,'RM374',5X,'RM375',5X,'RM376',5X,'RM377',5X,'RM378',5X,'RM379',5X,'RM380',5X,'RM381',5X,'RM382',5X,'RM383',5X,'RM384',5X,'RM385',5X,'RM386',5X,'RM387',5X,'RM388',5X,'RM389',5X,'RM390',5X,'RM391',5X,'RM392',5X,'RM393',5X,'RM394',5X,'RM395',5X,'RM396',5X,'
```

**Figure B.3 - Computer Code (continued)**

14/39/43

DATE = 77258

MAIN

```

PCSTRAN IV G LEVEL 21
0053      180  CONTINUE
0054      KPRINT=1
0055      200  CONTINUE
0056      GO TO 1
0057      210  STOP
0058      END
    
```

```

00701170
00301183
00001190
00001200
00301210
10001223
    
```

Figure B.3 - Computer Code (continued)

14/19/73

DATE = 77258

MODEP1

PCSTRAN IV G LEVEL 21

```

0001 SURROUTINE MODEP1(PMA,EPPL)
0002 COMMON/MODEP1/JJ,ALFAT(50),SCI,(SC,5),N(50),RC(50),ALFAT(50)
0003 DIMENSION A(10)
C THIS SUBROUTINE COMPUTES STANDARD DEVIATION BETWEEN R(J,K) AND S(I,J)
C FOR PI(K)
C WHERE
C R(I,J,K) EXPERIMENTAL BURNING RATE FOR JTH FORMULATION AT PI(K)
C RC(I,J) THEORETICAL BURNING RATE FOR JTH FORMULATION AT PI(K)
C RMA(I,J) BURNING RATE FOR ITH MODE OF FORMULATION AT PI(K)
C ALFAT(I,J) MASS FRACTION OF ITH MODE OX IN JTH FORMULATION
C ALFAT(I,J) TOTAL OX MASS FRACTION IN JTH FORMULATION
C II NUMBER OF OX MODES < 8
C JJ NUMBER OF FORMULATIONS < 50
C ERR(I,J) ERROR BETWEEN R(I,J,K) AND RC(I,J) AT PI(K)
C ERR1 STANDARD ERROR OF ESTIMATE FOR DATA SET R AND RC
C ROBERT LAIN GLICK AUGUST 3, 1977
C
10 ERR1=0.00
15 DO 30 J=1,JJ
   RC(J)=0.0
   DO 25 I=1,II
     RC(I,J)=RC(I,J)/ALFAT(I,J)*ABS(RMA(1))
   C COMPUTE ABSOLUTE ERROR
   C ERR(I,J)=R(I,J,K)-RC(I,J)
   C COMPUTE RELATIVE ERROR
   ERR(J)=(R(I,J,K)-RC(I,J))/P(J,K)
   ERR1=ERR1+ERR(J)*ERR(J)
30 CONTINUE
ERR1=SQRT(ERR1/JJ)
RETURN
END

```

Figure B.3 - Computer Code (continued)



14/30/43

DATE = 7725R

PATSH

FORTRAN IV G LEVEL 21

```

0001 SUBROUTINE PATSH(PSI,SSI,DEL,DELMIN,ITLIM,IPR,IPRT)
C THIS VERSION OF PATSH HAS BEEN ALTERED FROM THE MULTISZ VERSION TO
C CONFORM TO THE CALLING SEQUENCE OF THE ORIGINAL CODE ISFF WITH MULTIFIP
C COMMON/OPTIMN,DEL,DELMIN,ITLIM,IPR
C DIMENSION PSI(25),PMI(25),YMT(24),YF1(24)
C DATA IPR/6/
C DATA ALFA/1.02/
C FISSI=SSS-AR(SSSI)*.0001*GUT
C THE ITWICE PARAMETER ADDED BY MULTISZ HAS BEEN SPECIFICALLY
ITWICE=1
DEL=DELS
IF (IPR-GE.0) WRITE(IPR,604) DEL,DELMIN,ITLIM,IPR
DO 705 I=1,N
ITER=0
IFLGIT=1.
CUT=1.
10 CALL WRITE4(PSI,SSI)
90 SSIYST=FISSI
100 S=SSI
NPATM=0
DO 101 I=1,N
PMI(I)=PSI(I)
ICALL=1
IF (IPR-LE.0) GO TO 150
WRITE(IPR,599) ITER
WRITE(IPR,600) (PSI(J),J=1,N)
WRITE(IPR,601) S,DEL
GO TO 150
160 IF (S-LE.SSIYST) GO TO 200
DEL=DEL/2.
IF (DEL-GE.0) GO TO 100
IF (IPR-GE.0) WRITE(IPR,704)
IF (CUT-LE.5) GO TO 702
CALL WRITE4(PMI,SP1)
IF (IPR-GE.0) WRITE(IPR,707)
IF (ITWICE-EG.0) RETURN
DEL=DELS
CUT=0.
GO TO 90
200 SSI=S
SSIYST=FISSI
ITER=ITER+1
NPATM=NPATM+1
IF (ITER-GE.0) GO TO 700
IF (IPR-LE.0) GO TO 203
WRITE(IPR,599) ITER
WRITE(IPR,599) NPATM
WRITE (IPR,600) (PMI(I),I=1,N)
WRITE (IPR,601) SSI,DEL
IF (IPR-LE.0) GO TO 203
IPR=IPR+1
IPR=IPR+1
IF (IPR-GE.0) GO TO 100
CALL WRITE4(PSI,SP1)
IPR=IPR+1
IPR=IPR+1
C MAKE PATTERN MOVE

```

Figure B.3 - Computer Code (continued)



